LETTER

https://doi.org/10.1038/s41586-018-0118-y

RSPO2 inhibition of RNF43 and ZNRF3 governs limb development independently of LGR4/5/6

Emmanuelle Szenker-Ravi[1,17], Umut Altunoglu[2,17], Marc Leushacke[1,17], Célia Bosso-Lefèvre[1,3], Muznah Khatoo[1], Hong Thi Tran[4], Thomas Naert[4], Rivka Noelanders[4], Amin Hajamohideen[1], Claire Beneteau[5], Sergio B. de Sousa[6,7], Birsen Karaman[2], Xenia Latypova[5], Seher Başaran[2], Esra Börklü Yücel[8], Thong Teck Tan[1], Lena Vlaeminck[4,16], Shalini S. Nayak[9], Anju Shukla[9], Katta Mohan Girisha[9], Cédric Le Caignec[5,10], Natalia Soshnikova[11], Zehra Oya Uyguner[2], Kris Vleminckx[4]*, Nick Barker[1,12,13]*, Hülya Kayserili[2,8]* & Bruno Reversade[1,3,8,14,15]*

The four R-spondin secreted ligands (RSPO1–RSPO4) act via their cognate LGR4, LGR5 and LGR6 receptors to amplify WNT signalling[1–3]. Here we report an allelic series of recessive *RSPO2* mutations in humans that cause tetra-amelia syndrome, which is characterized by lung aplasia and a total absence of the four limbs. Functional studies revealed impaired binding to the LGR4/5/6 receptors and the RNF43 and ZNRF3 transmembrane ligases, and reduced WNT potentiation, which correlated with allele severity. Unexpectedly, however, the triple and ubiquitous knockout of *Lgr4*, *Lgr5* and *Lgr6* in mice did not recapitulate the known *Rspo2* or *Rspo3* loss-of-function phenotypes. Moreover, endogenous depletion or addition of exogenous RSPO2 or RSPO3 in triple-knockout *Lgr4/5/6* cells could still affect WNT responsiveness. Instead, we found that the concurrent deletion of *rnf43* and *znrf3* in *Xenopus* embryos was sufficient to trigger the outgrowth of supernumerary limbs. Our results establish that RSPO2, without the LGR4/5/6 receptors, serves as a direct antagonistic ligand to RNF43 and ZNRF3, which together constitute a master switch that governs limb specification. These findings have direct implications for regenerative medicine and WNT-associated cancers.

Limb development is governed by a three-dimensional signalling system that defines proximodistal, anteroposterior and dorsoventral axes[4]. Tetra-amelia with lung hypo/aplasia syndrome (TETAMS; MIM database entry 273395) is an extreme condition, in which fetuses lack all four limbs. TETAMS without lung hypoplasia has been linked to a *WNT3* nonsense mutation in humans[5]. The four R-spondin ligands (RSPO1–RSPO4) act as enhancers of WNT signalling[6–9]. They bind to their cognate receptors LGR4, LGR5 and LGR6 via their Furin-like 2 domain, and to the E3 ubiquitin ligases RNF43 and ZNRF3 via their Furin-like 1 domain[10]. This tripartite interaction prevents WNT receptor degradation mediated by RNF43 or ZNRF3. *Rspo2* mutation in mice leads to limb truncations reminiscent of tetra-amelia[11–14], but a role for its receptors has not been substantiated, to our knowledge, during limb morphogenesis.

Here, we describe five families with eleven affected individuals that display severe developmental limb defects. In family 1, four affected fetuses presented with radial ray deficiency with humeral involvement, absence of tibiae with or without femoral deficiency, and absence of digits on the preaxial side (Fig. 1a, b, Extended Data Fig. 1a and Extended Data Table 1). We propose to name this severe dysostosis humero-femoral hypoplasia with radio-tibial ray deficiency (HFH-RTRD). Exome sequencing identified a homozygous p.Arg69Cys mutation in *RSPO2* (Extended Data Fig. 1b) that affects a residue conserved in all R-spondin paralogues and homologues (Fig. 1c and Extended Data Fig. 2a). The analogous mutation p.Arg64Cys in *RSPO4* was shown to cause congenital anonchia[15]. The seven affected fetuses from families 2 to 5 presented with complete absence of four limbs, lung hypo/aplasia, cleft lip-palate, and labioscrotal fold aplasia, all characteristic of TETAMS (Fig. 1a, b, Extended Data Fig. 1a and Extended Data Table 1). A p.Gln70* nonsense mutation in *RSPO2* was identified in family 2[16] (Fig. 1a, c). In family 3[17], array comparative genomic hybridization (array-CGH) analysis identified a biallelic deletion of 154 kilobases (kb) spanning intron 5 and exon 6 of *RSPO2* (Fig. 1a, c and Extended Data Fig. 1c). In family 4, exome sequencing revealed a recessive p.Glu137* nonsense mutation in *RSPO2* (Fig. 1a, c). In family 5 with three consecutive TETAMS fetuses, a homozygous *RSPO2* frameshift p.Gly42Val fs*49 mutation was identified (Fig. 1a–c). These results establish a new aetiology for tetra-amelia and demonstrate the crucial involvement of RSPO2 in craniofacial, limb and lung development in humans.

We selected the p.Arg69Cys (R69C) and p.Gln70* (Q70X) mutations that are responsible for HFH-RTRD and TETAMS, respectively, to assess whether mutant RSPO2 retained binding to its cognate receptors. By co-immunoprecipitation analysis, only wild-type RSPO2, but not the RSPO2(F105A/F109A) mutant that specifically abrogates binding to LGRs[18], nor the RSPO2(R69C) or RSPO2(Q70X) mutants, was able to be pulled down by LGR5 (Fig. 1d and Extended Data Fig. 2b, c). Although the RSPO2(F105A/F109A) mutant could be readily co-immunoprecipitated by RNF43 or ZNRF3, neither RSPO2(R69C) nor RSPO2(Q70X) could interact with RNF43 or ZNRF3 (Fig. 1e and Extended Data Fig. 2d). Similarly, only wild-type RSPO2, but not the RSPO2(R69C) or RSPO2(Q70X) mutants, could be retained on the surface of HEK293T cells overexpressing LGR5 or RNF43 (Extended Data Fig. 2e). Wild-type RSPO2, and to a lesser extent RSPO2(R69C) but not RSPO2(Q70X), could enhance WNT3A-mediated activation of SUPERTOPFLASH (STF) luciferase (Fig. 1f and Extended Data Fig. 2f). These in vitro results indicate that the R69C and Q70X mutations diminish the ability of RSPO2 to bind to LGRs, RNF43 or ZNRF3, and to amplify β-catenin-dependent WNT signalling. These signalling defects correlate with the severity of the fetuses' phenotypes—the nonsense Q70X mutation (responsible for TETAMS) behaving as a null mutation, and the R69C mutation (responsible for HFH-RTRD) as a hypomorphic allele.

In mice, *Rspo2* is expressed in the apical ectodermal ridge of the growing limb and in the lung mesenchyme[11]. Accordingly, *Rspo2*

[1]Institute of Medical Biology, A*STAR, Singapore, Singapore. [2]Medical Genetics Department, Istanbul Medical Faculty, Istanbul University, Istanbul, Turkey. [3]Department of Paediatrics, National University of Singapore, Singapore, Singapore. [4]Department of Biomedical Molecular Biology, Ghent University, Ghent, Belgium. [5]CHU Nantes, Service de Génétique Médicale, Nantes, France. [6]Medical Genetics Unit, Hospital Pediátrico, Centro Hospitalar e Universitário de Coimbra, Coimbra, Portugal. [7]University Clinic of Genetics, Faculty of Medicine, University of Coimbra, Coimbra, Portugal. [8]Medical Genetics Department, Koç University School of Medicine (KUSOM), Istanbul, Turkey. [9]Department of Medical Genetics, Kasturba Medical College, Manipal University, Manipal, India. [10]INSERM, UMR1238, Bone Sarcoma and Remodeling of Calcified Tissue, Université Bretagne Loire, Nantes, France. [11]Institute of Molecular Biology (IMB) gGmbH, Mainz, Germany. [12]Cancer Research Institute, Kanazawa University, Kakuma-machi, Kanazawa, Japan. [13]Centre for Regenerative Medicine, The University of Edinburgh, Edinburgh, UK. [14]Institute of Molecular and Cellular Biology, A*STAR, Singapore, Singapore. [15]Reproductive Biology Laboratory, Academic Medical Center (AMC), Amsterdam-Zuidoost, The Netherlands. [16]Present address: Department of Plant Biotechnology and Bioinformatics, Ghent University, Ghent, Belgium. [17]These authors contributed equally: Emmanuelle Szenker-Ravi, Umut Altunoglu, Marc Leushacke.
*e-mail: kris.vleminckx@irc.ugent.be; nicholas.barker@imb.a-star.edu.sg; hkayserili@kuh.ku.edu.tr; bruno@reversade.com

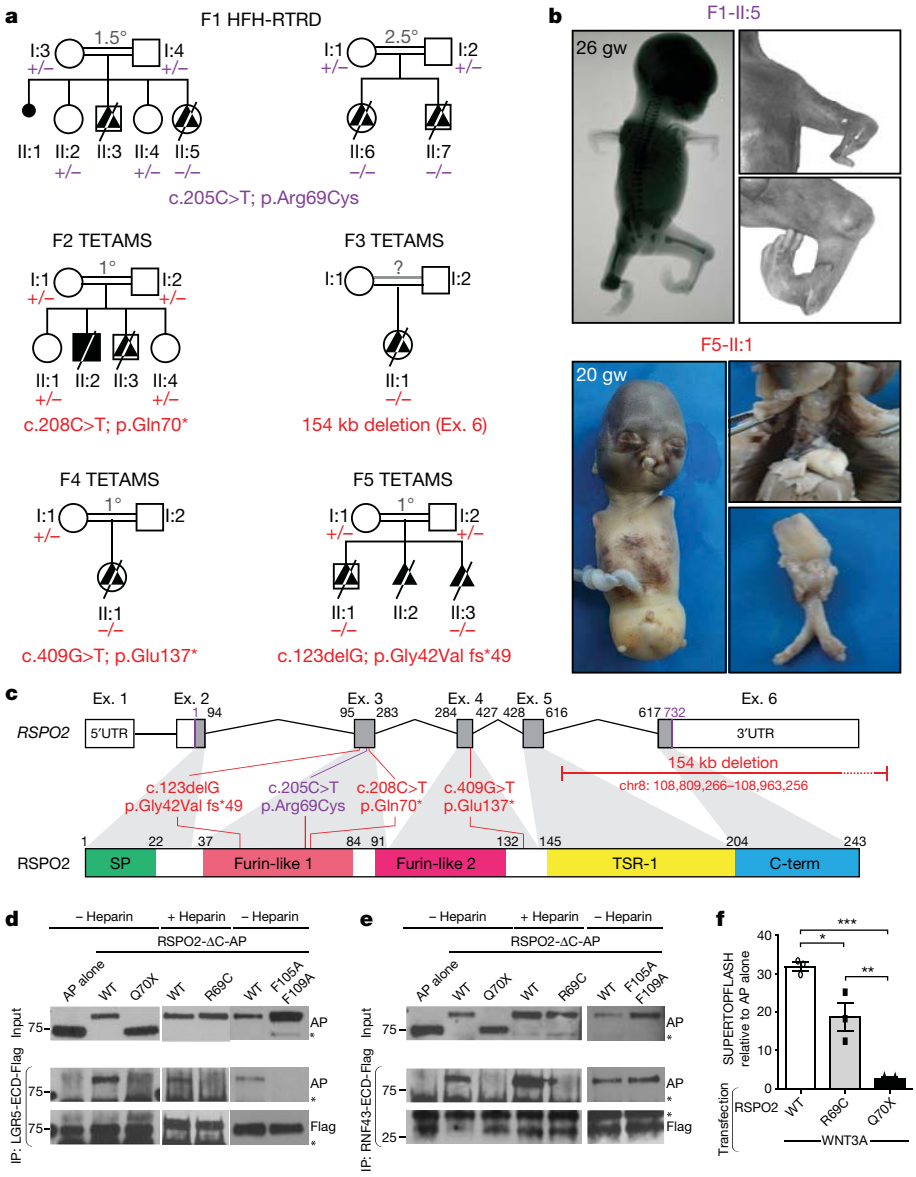

Fig. 1 | Identification of *RSPO2* mutations in fetuses presenting with severe limb defects. a, Pedigrees of family 1 (F1) with HFH-RTRD and families 2–5 (F2–F5) with TETAMS, and *RSPO2* germline mutation status for available family members. **b**, Pictures and radiographs illustrating limb defects in a fetus with HFH-RTRD, and complete absence of limbs and lungs in a fetus with TETAMS. gw, gestational weeks. **c**, *RSPO2* genomic (top) and protein (bottom) structures with identified mutations. Ex., exon. UTR, untranslated region. **d**, Co-immunoprecipitation (IP) of alkaline phosphatase (AP)-tagged RSPO2 lacking the C-terminal domain (ΔC; RSPO2-ΔC-AP) with Flag-tagged extracellular domains (ECD) of LGR5 (LGR5-ECD-Flag). WT, wild-type. **e**, Co-immunoprecipitation of RSPO2-ΔC-AP with RNF43-ECD-Flag. Asterisks indicate non-specific bands. Experiments in **d** and **e** were repeated three times. **f**, SUPERTOPFLASH assay in HEK293T-STF cells transfected with WNT3A and the indicated RSPO2 constructs. $n = 3$ biological replicates. Data are mean ± s.e.m. $^{*}P < 0.05$, $^{**}P < 0.01$, $^{***}P < 0.001$, one-way analysis of variance (ANOVA) with Bonferroni's correction. For gel source data, see Supplementary Fig. 1

homozygous mutant mice show lung hypoplasia and limb truncations[11–14]. Consistent with a reduction in canonical WNT signalling, these *Rspo2* phenotypes could be recapitulated in embryos born to gestating mice fed with a pan-WNT inhibitor[19] (Fig. 2a–d). Because individual *Lgr4*, *Lgr5* or *Lgr6* mutant mice[20–22] and *LGR4* or *LGR6* human knockout individuals[23,24] do not present any limb or lung phenotypes, we surmised that functional redundancy might exist between these three receptors. We therefore set to recapitulate TETAMS in mice by genetically deleting *Lgr4/5/6* in all embryonic tissues (Extended Data Fig. 4a). $Lgr4^{+/-}Lgr5^{+/-}Lgr6^{-/-}$ animals were inbred, yielding a 1 in 16 chance of obtaining triple-knockout *Lgr4/5/6* offspring (Extended Data Fig. 3a). Five triple-knockout *Lgr4/5/6* embryos were obtained at embryonic day (E) 14.5 or E18.5. Although they displayed the expected *Lgr4* and *Lgr5* phenotypes (Extended Data Fig. 4b–e)[20,21,25], none exhibited phenotypes reminiscent of tetra-amelia with lung agenesis (Fig. 2e–g and Extended Data Fig. 3b, c). This suggests that the LGR4, LGR5 and LGR6 receptors are not functionally redundant and do not mediate RSPO2 signalling for limb and lung morphogenesis. Other developmental phenotypes such as cleft palate[26] and ankyloglossia[21] were common between *Rspo2* and triple-knockout *Lgr4/5/6* embryos (Extended Data Figs. 3d, 4e, Extended Data Table 1). Notably, *Rspo3* knockout mouse embryos die at E10.5 owing to defective vascularization[27], a phenotype not seen in *Lgr4/5/6* triple-knockout embryos (Extended Data Fig. 3e). Thus, RSPO3-mediated vascularization is also LGR4/5/6-independent. These in vivo genetic findings suggest that RSPO2 and RSPO3 may engage other receptors for limb, lung and vascular development.

The expression of *Lgr4/5/6*, *Rnf43* and *Znrf3* could be examined in the recovered mutant embryos at E14.5. As expected, they had no *Lgr4* or *Lgr5* expression (Extended Data Fig. 5a–e). Some residual

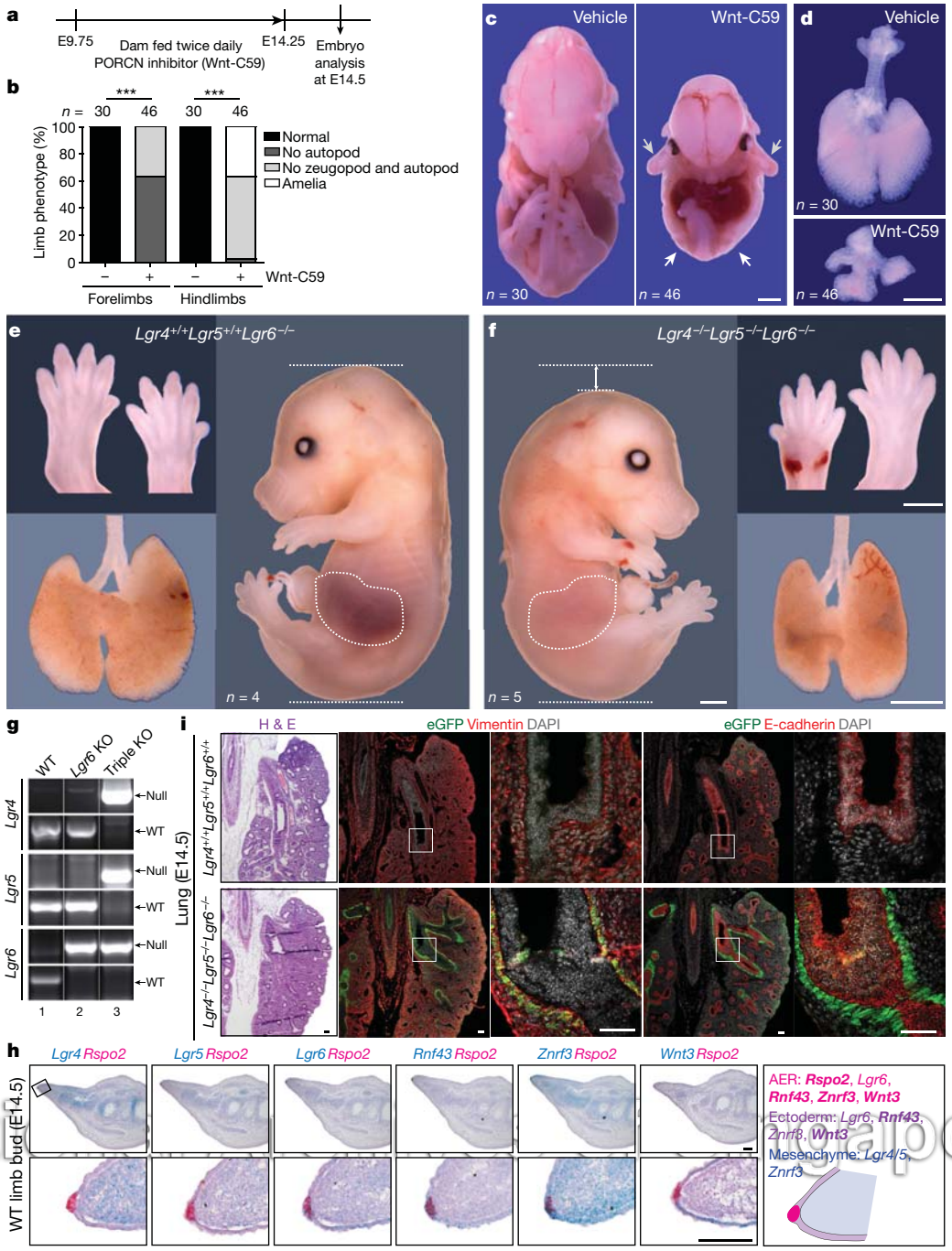

Fig. 2 | Mouse *Lgr4/5/6* triple-knockout embryos do not recapitulate the *Rspo2* and *Rspo3* phenotypes. a–d, PORCN inhibition using Wnt-C59 during embryogenesis leads to limb and lung defects. **a**, Experimental scheme. **b**, Scoring of limb phenotypes in vehicle-treated ($n = 30$) and Wnt-C59 treated ($n = 46$) embryos. ***$P < 0.001$, two-sided Fisher's exact test. **c**, Representative images of treated embryos. Grey (no zeugopod and autopod), and white (amelia) arrows denote limb defects. Scale bars, 1 mm. **d**, Representative images of lungs from treated embryos. Scale bar, 1 mm. **e–g**, Triple-knockout *Lgr4/5/6* does not lead to limb or lung defects. Representative photos of a *Lgr6* knockout ($n = 4$) (**e**) and a triple-null *Lgr4/5/6* ($n = 5$) (**f**) embryo at E14.5, with intact limbs and lungs. Dotted lines indicate the size difference and expected liver position. Scale bars, 1 mm. **g**, PCR-based genotyping. KO, knockout. **h**, Duplex RNAscope images for the indicated transcripts (blue) and *Rspo2* (pink) in transverse sections of wild-type forelimbs. AER, apical ectodermal ridge. Strongly expressed genes are denoted in bold (summary on the right). Scale bars, 0.1 mm. **i**, Haematoxylin and eosin (H&E) and antibody staining in coronal sections of wild-type (top) and triple-knockout (bottom) *Lgr4/5/6* lungs. Scale bars, 50 μm. Experiments in **h** and **i** were repeated three times

Lgr6 expression was observed, which may be originating from an alternative downstream methionine that would delete the LGR6 signal peptide[28]. During limb development, *Lgr4* and *Lgr5* were not expressed in the overlying ectoderm of the limb bud, whereas ectodermal *Lgr6* and *Wnt3* co-localized with *Rspo2* in the apical ectodermal ridge. The expression of *Znrf3* was ubiquitous, whereas *Rnf43* was restricted to the ectoderm (Fig. 2h). In developing lungs, robust *Lgr6* expression was detected in the smooth muscle cells (SMCs), whereas *Lgr4* and *Lgr5* were expressed at low levels in both the epithelium and mesenchyme lineages. *Znrf3* was ubiquitous and overlapped with *Rspo2* in the mesenchyme, whereas *Rnf43* expression was restricted to the lung epithelium (Extended Data Fig. 5f). Using the enhanced green fluorescent protein (eGFP) reporter of the *Lgr4/5/6* knock-in alleles (Extended Data Fig. 4a), we confirmed eGFP expression in a single

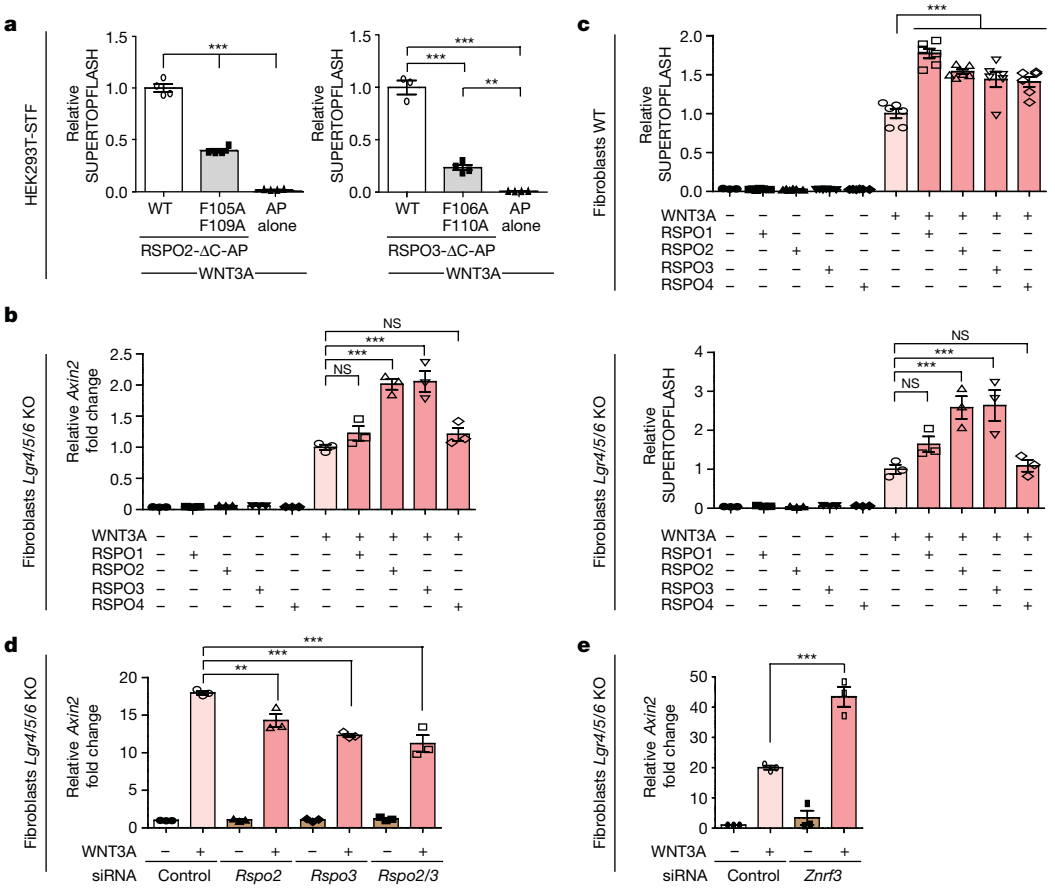

Fig. 3 | Exogenous and endogenous RSPO2/3 signal in *Lgr4/5/6* triple-knockout mouse embryonic fibroblasts. a, SUPERTOPFLASH assay in HEK293T-STF cells transfected with WNT3A and the indicated RSPO2 or RSPO3 constructs. $n = 4$ biological replicates. **b**, qPCR analysis for *Axin2* in *Lgr4/5/6* triple-knockout SV40-immortalized mouse fibroblasts treated with WNT3A and/or RSPO1–RSPO4. $n = 3$ biological replicates. **c**, SUPERTOPFLASH assay in wild-type (top, $n = 6$) and *Lgr4/5/6* triple-knockout (bottom, $n = 3$ biological replicates) SV40-immortalized mouse fibroblasts treated with WNT3A and/or RSPO1–RSPO4. **d**, **e**, qPCR analysis for *Axin2* in *Lgr4/5/6* triple-knockout SV40-immortalized mouse fibroblasts transfected with the indicated siRNAs, and treated with or without WNT3A. $n = 3$ biological replicates. Data are mean ± s.e.m. NS, not significant. $^{*}P < 0.05$, $^{**}P < 0.01$, $^{***}P < 0.001$, one-way ANOVA with Bonferroni's correction

layer of vimentin-positive cells adjacent to the E-cadherin-positive lung epithelium (Fig. 2i). In summary, these results demonstrate consistent co-expression of *Rspo2* with *Znrf3* at E14.5, whereas only partial overlap with *Lgr4/5/6* was seen.

We noticed that mutant RSPO2(F105A/F109A) and RSPO3(F106A/F110A), which cannot bind LGRs, are still able to enhance WNT signalling in HEK293T-STF cells (Fig. 3a). Neural progenitor cells (NPCs), induced pluripotent stem (iPS) cells and SV40-immortalized dermal fibroblasts were derived from E14.5 wild-type and mutant embryos to test the activity of exogenous and endogenous R-spondin ligands in triple *Lgr4/5/6*-null cells (Extended Data Fig. 6a–c). Recombinant RSPO2 and RSPO3, but not RSPO1 and RSPO4, could still amplify WNT3A-mediated signalling in *Lgr4/5/6* triple-knockout immortalized STF-fibroblasts (Fig. 3b, c). Most importantly, short interfering RNA (siRNA)-mediated depletion of endogenous *Rspo2* or *Rspo3* was sufficient to significantly decrease expression of the WNT direct target gene *Axin2* in WNT3A-treated *Lgr4/5/6* triple-knockout fibroblasts. This may be explained by RSPO2 and RSPO3 inhibition of ZNRF3, because siRNA-depletion of endogenous *Znrf3* resulted in increased endogenous *Axin2* expression (Fig. 3d, e and Extended Data Fig. 6d). These in vitro data support our in vivo results, and confirm that cells that lack LGR4/5/6 are still sensitive to RSPO2/3-mediated WNT signalling enhancement. Similar observations were made in human haploid cells mutant for LGR4/5/6[29].

To further validate the causal link between RSPO2 deficiency and amelia, we unilaterally injected *rspo2* guide RNA (gRNA) with Cas9 protein into *Xenopus tropicalis* embryos at the two-cell stage (Fig. 4a). Targeted next-generation sequencing and BATCH-GE analysis demonstrated very high in vivo efficiencies for *rspo2* deletions (Supplementary Table 1), which caused marked unilateral forelimb and hindlimb amelia (Fig. 4b, d). Because we showed in mice that LGR4, LGR5 and LGR6 are not involved in limb development, we examined RNF43 and ZNRF3, which may serve as alternative cell-surface RSPO2 receptors. The use of *Xenopus* allows us to bypass a possible mammalian-specific RNF43 and ZNRF3 requirement for placental vascularization. Both ligases were uniformly expressed in developing limb buds (Fig. 4c). Two TALEN pairs for each gene were selected for their very high cutting efficiency (Supplementary Table 1). Although limb defects were rare, or absent, within single *rnf43* or *znrf3* mutants, unilateral ectopic limbs were very prominent in *znrf3/rnf43* double-mutant frogs (Fig. 4d–h). Alizarin red and alcian blue staining revealed a diverse spectrum of limb phenotypes ranging from diplopodia to complete polymelia, with bifurcations arising at distinct locations across the stylopod, zeugopod or autopod. Extreme cases presented up to quadruplication of forelimbs (Fig. 4h and Extended Data Fig. 7b), a phenotype that is the inverse of *rspo2* crispant frogs that display total amelia (Extended Data Fig. 7a). We conclude that in the context of limb development, RSPO2 behaves as a direct antagonistic ligand to RNF43 and ZNRF3 without the need for LGR4/5/6. This ligand–receptor pair constitutes a master switch that governs the number of limbs an embryo should form. It will be important to assess whether this pathway can in part contribute to the disappearance of limbs during evolution, particularly in cetaceans and snakes, which are tetrapods that have become bi-amelic and tetra-amelic, respectively. It is also tempting to speculate whether the same

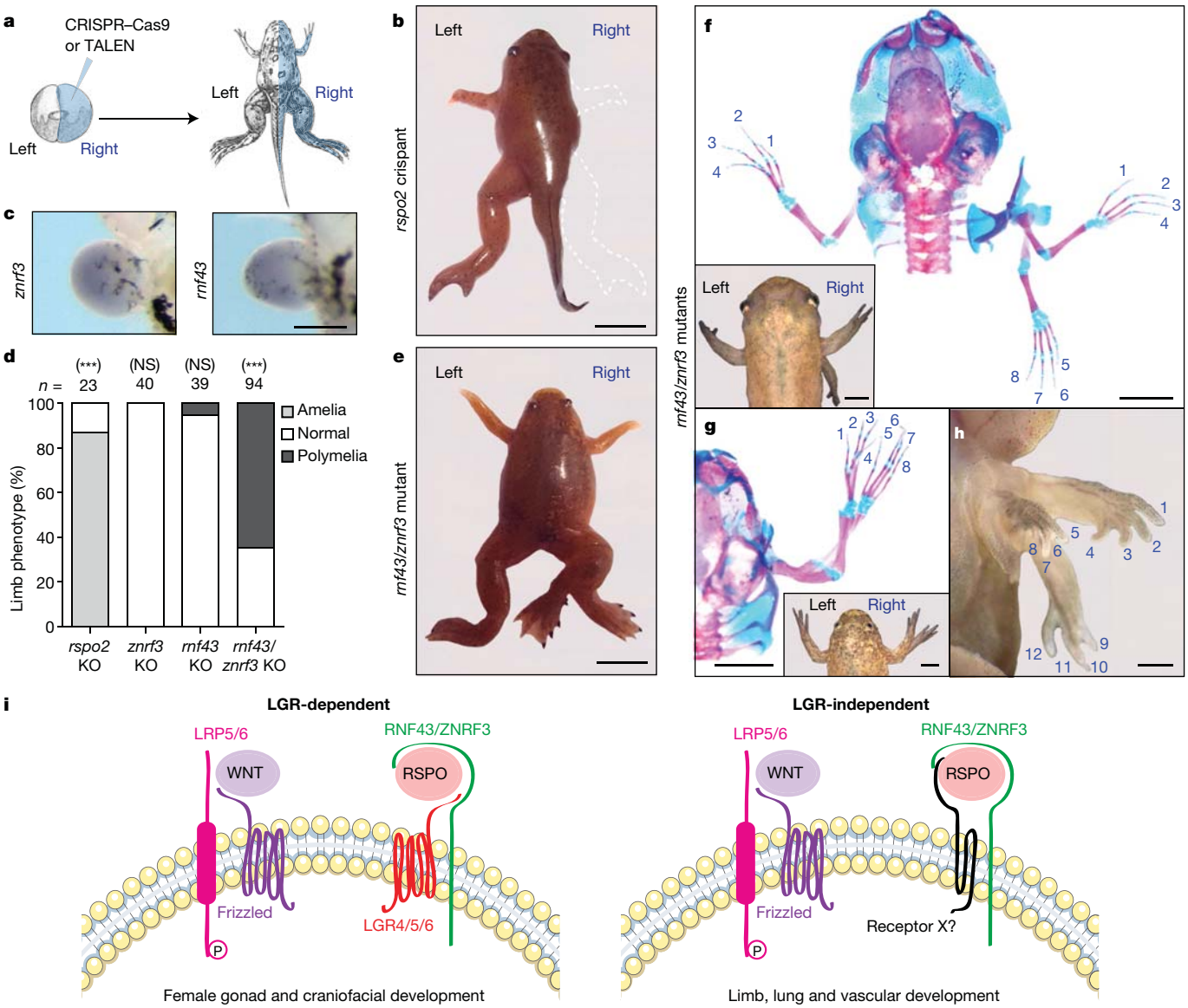

Fig. 4 | Frogs mutant for both *rnf43* and *znrf3* display complete limb duplications. a, Experimental scheme using *X. tropicalis*. **b**, Representative *rspo2* crispant (stage 63; $n = 21$). Scale bar, 0.5 cm. **c**, *znrf3* and *rnf43* in situ hybridization in stage 50 limb buds. Scale bar, 300 μm. The experiment was repeated three times. **d**, Scoring of limb phenotype. *n* denotes number of froglets. NS, not significant; $***P < 0.001$, significantly different from normal (χ^2 test). **e**, Stage 67 *znrf3/rnf43* double mutant with a duplicated right hindlimb. Scale bar, 0.5 cm. **f**, **g**, External view and alizarin red and alcian blue staining of *rnf43/znrf3* double mutants (stages 62 (**f**) and 66 (**g**)). Scale bars, 0.3 cm. **h**, *rnf43/znrf3* double-mutant tadpole (stage 59) displaying quadruplication of the right forelimb (three are visible). Scale bar, 0.2 cm. In **e**–**h**, 61 *znrf3/rnf43* double-mutant froglets with polymelia were obtained. **i**, Updated model for LGR-dependent R-spondin processes (left), and LGR-independent RSPO2/3 signalling (right), which may involve the activity of a hitherto unknown receptor X

embryonic signals may be re-mobilized in salamanders, which are capable of complete adult limb regeneration after amputation[30].

The current model suggests that RSPO–LGR form ligand–receptor pairs that serve to increase WNT signalling through direct inhibition of the two E3 ligases RNF43 and ZNRF3, which otherwise ubiquitinate WNT receptors for degradation[31,32]. Here we challenge this view and show that during embryogenesis, the concomitant loss of LGR4, LGR5 and LGR6 receptors does not phenocopy the loss of RSPO2 or RSPO3 (Fig. 4i).

Gain-of-function variants in *RSPO2* and *RSPO3* and loss-of-function alleles in *RNF43* and *ZNRF3* are the most frequent somatic mutations in colorectal cancer patients[33,34]. *LGR5*-positive cells have been shown to represent the major cell of origin of colorectal cancer[35]; however, pathogenic mutations in this WNT-associated receptor have not been documented so far. Our findings that RSPO2 and RSPO3 can inhibit RNF43 and ZNRF3, without the need for LGR4/5/6, raise the question of whether LGRs have any functional relevance to carcinogenesis. The ubiquitous triple-knockout *Lgr4/5/6* during embryogenesis serves as a proof-of-concept for subsequent organ-specific deletions, and should enable this question to be addressed.

Online content

Any Methods, including any statements of data availability and Nature Research reporting summaries, along with any additional references and Source Data files, are available in the online version of the paper at https://doi.org/10.1038/s41586-018-0118-y.

Received: 9 November 2016; Accepted: 10 April 2018;
Published online: 16 May 2018

1. de Lau, W. et al. Lgr5 homologues associate with Wnt receptors and mediate R-spondin signalling. *Nature* **476**, 293–297 (2011).
2. Glinka, A. et al. LGR4 and LGR5 are R-spondin receptors mediating Wnt/β-catenin and Wnt/PCP signalling. *EMBO Rep.* **12**, 1055–1061 (2011).

3. Carmon, K. S., Gong, X., Lin, Q., Thomas, A. & Liu, Q. R-spondins function as ligands of the orphan receptors LGR4 and LGR5 to regulate Wnt/β-catenin signaling. *Proc. Natl Acad. Sci. USA* **108**, 11452–11457 (2011).
4. Niswander, L. Pattern formation: old models out on a limb. *Nat. Rev. Genet.* **4**, 133–143 (2003).
5. Niemann, S. et al. Homozygous WNT3 mutation causes tetra-amelia in a large consanguineous family. *Am. J. Hum. Genet.* **74**, 558–563 (2004).
6. Kazanskaya, O. et al. R-Spondin2 is a secreted activator of Wnt/β-catenin signaling and is required for *Xenopus* myogenesis. *Dev. Cell* **7**, 525–534 (2004).
7. Kim, K. A. et al. R-Spondin proteins: a novel link to β-catenin activation. *Cell Cycle* **5**, 23–26 (2006).
8. Nam, J. S., Turcotte, T. J., Smith, P. F., Choi, S. & Yoon, J. K. Mouse cristin/R-spondin family proteins are novel ligands for the Frizzled 8 and LRP6 receptors and activate β-catenin-dependent gene expression. *J. Biol. Chem.* **281**, 13247–13257 (2006).
9. Ohkawara, B., Glinka, A. & Niehrs, C. Rspo3 binds syndecan 4 and induces Wnt/PCP signaling via clathrin-mediated endocytosis to promote morphogenesis. *Dev. Cell* **20**, 303–314 (2011).
10. Zebisch, M. et al. Structural and molecular basis of ZNRF3/RNF43 transmembrane ubiquitin ligase inhibition by the Wnt agonist R-spondin. *Nat. Commun.* **4**, 2787 (2013).
11. Bell, S. M. et al. R-spondin 2 is required for normal laryngeal-tracheal, lung and limb morphogenesis. *Development* **135**, 1049–1058 (2008).
12. Aoki, M., Kiyonari, H., Nakamura, H. & Okamoto, H. R-spondin2 expression in the apical ectodermal ridge is essential for outgrowth and patterning in mouse limb development. *Dev. Growth Differ.* **50**, 85–95 (2008).
13. Nam, J. S. et al. Mouse R-spondin2 is required for apical ectodermal ridge maintenance in the hindlimb. *Dev. Biol.* **311**, 124–135 (2007).
14. Yamada, W. et al. Craniofacial malformation in R-spondin2 knockout mice. *Biochem. Biophys. Res. Commun.* **381**, 453–458 (2009).
15. Brüchle, N. O. et al. RSPO4 is the major gene in autosomal-recessive anonychia and mutations cluster in the furin-like cysteine-rich domains of the Wnt signaling ligand R-spondin 4. *J. Invest. Dermatol.* **128**, 791–796 (2008).
16. Başaran, S. et al. Tetra-amelia, lung hypo-/aplasia, cleft lip-palate, and heart defect: a new syndrome? *Am. J. Med. Genet.* **51**, 77–80 (1994).
17. Sousa, S. B. et al. Tetra-amelia and lung hypo/aplasia syndrome: new case report and review. *Am. J. Med. Genet. A.* **146A**, 2799–2803 (2008).
18. Xie, Y. et al. Interaction with both ZNRF3 and LGR4 is required for the signalling activity of R-spondin. *EMBO Rep.* **14**, 1120–1126 (2013).
19. Proffitt, K. D. et al. Pharmacological inhibition of the Wnt acyltransferase PORCN prevents growth of WNT-driven mammary cancer. *Cancer Res.* **73**, 502–507 (2013).
20. Mazerbourg, S. et al. Leucine-rich repeat-containing, G protein-coupled receptor 4 null mice exhibit intrauterine growth retardation associated with embryonic and perinatal lethality. *Mol. Endocrinol.* **18**, 2241–2254 (2004).
21. Morita, H. et al. Neonatal lethality of LGR5 null mice is associated with ankyloglossia and gastrointestinal distension. *Mol. Cell. Biol.* **24**, 9736–9743 (2004).
22. Snippert, H. J. et al. Lgr6 marks stem cells in the hair follicle that generate all cell lineages of the skin. *Science* **327**, 1385–1389 (2010).
23. Styrkarsdottir, U. et al. Nonsense mutation in the *LGR4* gene is associated with several human diseases and other traits. *Nature* **497**, 517–520 (2013).
24. Sulem, P. et al. Identification of a large set of rare complete human knockouts. *Nat. Genet.* **47**, 448–452 (2015).
25. Koizumi, M. et al. Lgr4 controls specialization of female gonads in mice. *Biol. Reprod.* **93**, 90 (2015).
26. Jin, Y. R., Turcotte, T. J., Crocker, A. L., Han, X. H. & Yoon, J. K. The canonical Wnt signaling activator, R-spondin2, regulates craniofacial patterning and morphogenesis within the branchial arch through ectodermal-mesenchymal interaction. *Dev. Biol.* **352**, 1–13 (2011).
27. Aoki, M. et al. R-spondin3 is required for mouse placental development. *Dev. Biol.* **301**, 218–226 (2007).
28. van de Glind, G. C. et al. RNA-seq analysis of Lgr6^{+} stem cells and identification of an Lgr6 isoform. *Exp. Dermatol.* https://doi.org/10.1111/exd.13453 (2017).
29. Lebensohn, A. M. & Rohatgi, R. R-spondins can potentiate WNT signaling without LGRs. eLife 7, e33126 (2018).
30. Simon, A. & Tanaka, E. M. Limb regeneration. *Wiley Interdiscip. Rev. Dev. Biol.* **2**, 291–300 (2013).
31. Hao, H. X. et al. ZNRF3 promotes Wnt receptor turnover in an R-spondin-sensitive manner. *Nature* **485**, 195–200 (2012).
32. Koo, B. K. et al. Tumour suppressor RNF43 is a stem-cell E3 ligase that induces endocytosis of Wnt receptors. *Nature* **488**, 665–669 (2012).
33. Seshagiri, S. et al. Recurrent R-spondin fusions in colon cancer. *Nature* **488**, 660–664 (2012).
34. Bond, C. E. et al. RNF43 and ZNRF3 are commonly altered in serrated pathway colorectal tumorigenesis. *Oncotarget* **7**, 70589–70600 (2016).
35. Barker, N. et al. Crypt stem cells as the cells-of-origin of intestinal cancer. *Nature* **457**, 608–611 (2009).

Acknowledgements We are grateful to the families of affected fetuses whose cooperation made this study possible. We thank M. Krahn and D. Bertola for contributing more families with TETAMS for ongoing research. We thank C. Niehrs for the RSPO2-ΔC-AP-PCS2+construct. We thank D. Virshup for HEK293T-STF cells. The TALEN plasmids were obtained from C. H. K. Cheng. We are grateful to our groups' members for discussion and advice. E.S.-R. thanks M. Ravi for her patience and support, and is supported by a BMRC Young Investigator Grant (1613851035). S.S.N. is a recipient of Senior Research Fellowship from Indian Council of Medical Research (45/10/2015-HUM-BMS). N.B. is funded by A*STAR and an NRF Investigatorship. B.R. is a fellow of the Branco Weiss Foundation, an A*STAR Investigator, a NRF and AAA fellow and a Young EMBO Investigator. This work was partly funded by the Department of Science and Technology, India, for the project 'Application of autozygosity mapping and exome sequencing to identify genetic basis of disorders of skeletal development' (SB/SO/HS/005/2014); by the Research Foundation, Flanders (FWO-Vlaanderen) (grants G0A1515N and G029413N), the Concerted Research Actions from Ghent University (BOF15/GOA/01) and the Hercules Foundation, Flanders (grant AUGE/11/14), Belgium; by TUBITAK 108S412 and 112S398 (ERA-Net consortiums, CRANIRARE and CRANIRARE2), Turkey; and by a Strategic Positioning Fund on Genetic Orphan Diseases from A*STAR, Singapore.

Reviewer information *Nature* thanks C. Niehrs, C. Tabin and the other anonymous reviewer(s) for their contribution to the peer review of this work.

Author contributions The recruitment of families 1 and 2 and the initial discovery of *RSPO2* mutations were made by the team of H.K. with the help of U.A. and Z.O.U. Further patient data and samples were collected by H.K. from S.B.d.S., S.S.N., A.S. and K.M.G., who provided TETAMS families 3 and 5. C.B., X.L. and C.L.C. independently identified a *RSPO2* mutation in family 4. E.S.-R., M.L., K.V., N.S. and B.R. designed functional studies. N.B. provided single *Lgr4*, *Lgr5* and *Lgr6* knock-in mouse lines. E.S.-R., U.A., C.B., B.K., X.L., S.B., E.B.Y., C.L.C. and Z.O.U. performed whole-exome sequencing, chromosomal array analysis and sequencing analysis. E.S.-R., M.L., C.B.-L., M.K., H.T.T., T.N., R.N., A.H., N.S., T.T.T. and L.V. performed functional experiments. C.B.-L., M.K. and H.T.T. contributed equally to this work. E.S.-R., U.A., M.L., K.V., H.K. and B.R. wrote and revised the manuscript.

Competing interests The authors declare no competing interests.

Additional information
Extended data is available for this paper at https://doi.org/10.1038/s41586-018-0118-y.
Supplementary information is available for this paper at https://doi.org/10.1038/s41586-018-0118-y.
Reprints and permissions information is available at http://www.nature.com/reprints.
Correspondence and requests for materials should be addressed to K.V. or N.B. or H.K. or B.R.
Publisher's note: Springer Nature remains neutral with regard to jurisdictional claims in published maps and institutional affiliations.

METHODS

Fetuses and clinical assessment. The five families included in this study were enrolled from genetic departments of Istanbul, Turkey; Coimbra, Portugal; Nantes, France; and Mangalore, India. Eight out of eleven affected individuals had been clinically and radiologically evaluated by experienced clinical geneticists. Autopsy was performed in five cases (see Extended Data Table 1). Families 2 and 3 had been previously reported[16,17]. Written informed consent in accordance with the Helsinki protocol was obtained from family members before inclusion to the research protocol. Consent to publish photos was obtained from the families. The studies were performed in compliance with all relevant ethical regulations from the respective institutions. Approvals were obtained from the Istanbul University, Istanbul Medical Faculty ethical committee, Turkey (CRANIRARE: 2008/1194 and CRANIRARE-II: 2012/743-1061) as well as the Koç University School of Medicine (KUSoM) ethical committee, Istanbul, Turkey (2015.120.IRB2.047 CRANIRARE-2) for families 1 and 2; from the 'Comissão de Ética do Centro Hospitalar de Coimbra', Coimbra, Portugal (2009/42, 1724/Sec) for family 3; from the 'Comite de protection des personnes Ouest IV', Nantes, France (DC-2011-1399) for family 4; and from the institutional ethics committee of Kasturba Hospital, Manipal, India (ECR/146/Inst/KA/2013, IEC 430/2013) for family 5.

Genotyping and exome sequencing. DNA was extracted from skin biopsy samples of affected cases and from peripheral blood leukocytes of parents and healthy siblings by standard procedures. Affected individuals, or parents in the absence of samples from the affected individuals, were previously screened and excluded for any functional sequence variations/mutations in the *WNT3* (NM_030753) and *WNT7A* (NM_004625) genes. Whole-exome capture of subjects II:6 and II:7 from family 1 were performed using Agilent SureSelect Human All Exon v4.0 kit, sequenced on Illumina HiSeq2000 platform using TruSeq v3 chemistry at a mean coverage of 50 ×, reads provided in Fastq files were mapped to human genome (hg19) using Burrows–Wheeler Aligner (BWA package version 0.6.2). Local realignment was performed by Genome Analysis Tool Kit (GATK). Duplicated reads were marked for exclusion from further analysis using Picard (version 1.83) tool. Further alignment manipulations were performed by Samtools (version 0.1.18). Base quality (Phred scale) scores were recalibrated using the GATK covariance recalibration for each sample (Oxford Gene Technology), and variant calling was performed using ANNOVAR tool with avSNP release of 142, 1,000 genomes release of 2014 along with NIH-NHLBI 6500 exome database version 2. All the alterations including overlapping homozygous variants complying with minimum of 20 read depths were considered for further evaluation and browsed on OGT NGS (Oxford Gene Technologies' Next Generation Sequencing) and IGV (Integrated Genomic Viewer) browsers. Screening for *RSPO2* mutations in additional affected individuals or parents, and segregation validation were performed by Sanger sequencing, with PCR primers designed to cover all the coding exons and the flanking regions according to RefSeq accession number NM_178565 (Extended Data Table 2a).

Array-CGH and SNP-array analysis. Oligonucleotide array-CGH was performed using SurePrint G3 Human CGH Microarray ISCA 4 × 180 K v2 (Agilent Technologies), and the SNP-Array adopted was 300 K HumanCytoSNP-12v2-1 (Illumina Inc.). The 180 K kit has an overall median probe spacing of 13 kb, and the SNP-Array has 6.2 kb. Analyses were performed according to the protocols provided by the suppliers (Agilent Oligonucleotide Array-Based CGH for Genomic DNA Analysis and Illumina Karyostudio & Bluefuse Multi Softwares). Arrays were scanned using a NimbleGen MS 200 for Agilent SurePrint array and I-Scan instrument for HumanCytoSNP-12v2-1. Genomic positions were based on the UCSC February 2009 human reference sequence (hg19) (NCBI build 37 reference sequence assembly).

Constructs. An RSPO2-ΔC-AP-pCDNA3 plasmid (gift from C. Niehrs) encoding the wild-type human *RSPO2* open-reading frame (ORF) without the C-terminal domain (ΔC) (NP_848660 amino acids 1–206) tagged with alkaline phosphatase (AP) was used to generate the RSPO2-ΔC-AP R69C and F105A/F109A mutant constructs (RSPO2(R69C) and RSPO2(F105A/F109A)) using the QuikChange Mutagenesis Kit (Stratagene 200522). R69C is the missense mutation found in family 1, and the F105A/F109A mutations specifically abolish the interaction of RSPO2 with the LGRs[36,37]. RSPO2-Δ70-AP (RSPO2(Q70X), mutation found in family 2) was obtained by PCR and ligation (deleting the C-terminal region of the protein downstream of position 69). Deletion of the RSPO2 C-terminal domain (RSPO2-ΔC) decreases its retention on the cell surface without affecting its receptor binding and WNT enhancement properties[38]. A construct for a secreted alkaline phosphatase was used as a negative control. For cell surface binding assay experiments, V5-LGR5-pCS2 + (gift from C. Niehrs[2]), and pCMV6-Entry-RNF43 (Origene RC214013) plasmids were used. For co-immunoprecipitation experiments, the signal peptide and extracellular domains (ECD) of LGR5 (NP_001264156 amino acids 1–557), ZNRF3 (NP_001193927 amino acids 1–219), and RNF43 (NP_060233 amino acids 1–197) were subcloned in pCS2 + with a Flag tag at their C terminus.

HEK293T and HEK293T-STF cell culture. HEK293T (from ATCC) and HEK293T-STF (SUPERTOPFLASH, gift from D. Virshup, from ATCC) cell lines have not been authenticated but were tested negative for mycoplasma contamination. They were cultured on plates coated with poly-L-lysine (Sigma P4707) with the following medium: DMEM High glucose (HyClone SH30081.01) with 10% fetal bovine serum (Thermo Scientific SH30070), and 2 mM L-glutamine (ThermoFisher Scientific 25030081). Cells were transfected with DNA plasmid using the FuGENE HD Transfection Reagent (Promega E2312) in OptiMEM medium (Gibco 31985070).

Expression and secretion studies. For protein extraction, HEK293T cells were lysed using appropriate amount of RIPA buffer (Tris-HCl pH7.5, 50 mM, NaCl 150 mM, NP-40 0.1%, Na^{2+}-deoxycholate 0.05%) supplemented with proteinase inhibitors (Complete, Roche 04693159001). Lysates were centrifuged at 17,000*g* for 15 min at 4 °C to remove cell debris, and the supernatants (protein extracts) were collected. For secretion studies, culture medium was changed 24 h after transfection with a serum-free medium Pro293a-CDM (Lonza 12-764Q) supplemented with L-glutamine without or with 50 μg ml^{-1} of heparin (Sigma H3149). Secretion was allowed for 48 h before collection of the conditioned media. For western blotting, samples were electrophoresed with reducing Laemeli loading buffer after denaturation at 95 °C for 10 min. The protein ladder (Bio-Rad 161-0377) and denatured and reduced samples were loaded onto 4–20% gradient precast gels (BioRad Criterion 567-1093) in 1 × running buffer (25 mM Tris, 200 mM glycine, 0.1% SDS) and ran at 80–180 V until desired separation. Gels were transferred onto 0.2 μm PVDF membranes (BioRad Criterion 170-4157) using the Trans-Blot TurboTM transfer system for 7 min. Membranes were blocked for 1 h at room temperature with 5% milk in TBST (50 mM Tris-HCl pH 7.5, 150 mM NaCl; with 0.05% Tween20). Membranes were incubated with primary antibody diluted in 5% milk in TBST at 4 °C overnight (anti-alkaline phosphatase, 1:2,000, GenHunter Q310; anti-Flag, 1:1,000, Cell Signaling 14793 S; anti-GAPDH, 1:4,000, SantaCruz 47724). After washes in TBST, membranes were incubated for 1 h at room temperature with secondary antibodies (Mouse-HRP 71503510 or Rabbit-HRP 711035152, 1:4,000, Jackson Immuno) in 5% milk in TBST. After several washes in TBST, the signal was revealed with the HRP substrate (Thermo Scientific SuperSignal 34080/34076/34096) for 3 min at room temperature. Membranes were then exposed to CL-Xposure films (Thermo Scientific 34091), and developed in a Carestream Kodak developer.

Co-immunoprecipitation experiments. Conditioned media containing either of the RSPO2-ΔC-AP forms or the different receptor-ECD-Flag proteins were obtained after transfection in HEK293T. Conditioned media with equivalent amount of each RSPO2-ΔC-AP forms were first mixed with conditioned medium containing the receptor-ECD-Flag of interest for 4 h at 4 °C. At the same time, Protein G Dynabeads (Novex 10003D) were conjugated with anti-Flag antibodies (Sigma F3165) for 4 h at 4 °C. The media mixes (inputs) were then incubated with the conjugated beads overnight at 4 °C. After washes, the beads were re-suspended with 2 × reducing Laemeli loading buffer. After centrifugation, the supernatants (immunoprecipitants) were subsequently used for western blotting.

Cell-surface binding assay. Twenty-four hours after transfection of HEK293T cells with V5-LGR5-pCS2 + (gift from C. Niehrs[2]), pCMV6-Entry-RNF43 (Origene RC214013) or pCS2 + (empty vector) in 24-well plates, the cell culture medium was replaced for 3 h with 300 μl of conditioned medium containing equivalent amounts of RSPO2-ΔC-AP proteins (as determined by western blot), to assess for their cell-surface binding. After washes with PBS, cells were lysed with PBS containing Triton X-100 1% and 1 × proteinase inhibitor, and then incubated at 65 °C for 1 h to inhibit endogenous alkaline phosphatase activity. After centrifugation at 17,000*g* for 2 min, supernatants (protein extracts) were collected and the protein concentration was measured (Pierce BCA protein assay kit 23225). Eighty microlitres of the same quantity of total proteins for each condition was added to 80 μl of BM Purple (Roche 11442074001) and incubated overnight at 4 °C in the dark for chromogenic development. Pictures were taken with the NCS Microtek Artixscan F1 scanner.

SUPERTOPFLASH luciferase assay. HEK293T-STF cells were transfected with the human *WNT3A* gene (hWNT3A-pCS2 +) and the *Renilla* luciferase (pRL-CMV vector). RSPO2-ΔC-AP constructs were either transfected or conditioned media was added 24 h after transfection for another 24 h incubation. The expression of the firefly (STF) and *Renilla* luciferases were measured using the Dual-Luciferase Reporter Assay system (Promega E1960) 48 h after transfection. Measurements were done on opaque 96-well plates using a luminometer. Luminescence data are represented as the firefly luminescence relative to the *Renilla* luminescence and total protein concentration. Plotted are the values relative to the values for WNT3A plus alkaline phosphatase alone. For SV40-immortalized mouse fibroblasts-STF, cells were treated for 24 h with recombinant proteins re-suspended in PBS containing 0.1% BSA. Luminescence data are represented as the firefly luminescence relative to total protein concentration. Plotted are the values relative to the values for WNT3A alone. Data are average of three independent experiments and

statistical analyses were done using the PRISM5 software using a one-way ANOVA test with Bonferroni correction for multiple hypothesis testing. Not significant indicates $P > 0.05$. *$P < 0.05$, **$P < 0.01$ and ***$P < 0.001$. Error bars indicate s.e.m.

Mouse lines. All experiments on mice were executed in accordance with the guidelines and regulations of the respective institutions. Approvals were obtained in Singapore by the Institutional Animal Care and Use Committee (IACUC 140907, 171263, and 171210) and in Germany by the ethical committee of the Institute of Molecular Biology (IMB) gGmbH (permit number 23-177-07/G 16-05-071E1). *Lgr4-eGFP-ires-creERT2, Lgr5-eGFP-ires-creERT2* and *Lgr6-eGFP-ires-creERT2* mice have been described previously[1,22,39]. We incrossed $Lgr4^{+/-}Lgr5^{+/-}Lgr6^{-/-}$ animals and analysed 82 embryos (63 embryos at E14.5, and 19 embryos at E18.5, both male and female). See Extended Data Table 2b for the genotyping PCR primers used. For Porcupine inhibitor treatments, Wnt-C59 (Tocris, 5148/10) or vehicle (PBS containing 0.5% methylcellulose, 0.01% Tween-20, and 5% DMSO) was orally administered to wild-type pregnant females at 5 μg g^{-1} dam body weight every 12 h between E9.75 and E14.25, and embryos were collected at E14.5. We analysed a total of 30 embryos from vehicle-treated mothers, and 46 embryos from Wnt-C59-treated mothers. No statistical method was used to predetermine sample size. No randomization or blinding was used during the experimental procedures.

Mouse embryos sections. Embryos were fixed overnight at 4 °C in 4% paraformaldehyde and stored in 70% ethanol at 4 °C. For H&E staining, RNAscope and immunofluorescence experiments, embryos were subsequently paraffin-embedded and sectioned using a Leica RM2255 microtome. H&E staining was performed on deparaffinized and rehydrated 6 μm tissue sections according to standard protocols, and images were taken with the MetaSystems Metafer Slide Scanner. RNAscope experiments were performed on deparaffinized and rehydrated 6 μm tissue sections using the RNAscope 2.5 HD Duplex Assay (Advanced Cell Diagnostics ACD 322430). The ACD RNAscope probes used in this study are as follow: Mm-Rspo2-C2 (402001-C2), Mm-Lgr4 (318321), Mm-Lgr5 (312171), Mm-Lgr6 (404961), Mm-Rnf43 (400371), Mm-Znrf3 (434201), Mm-Wnt3 (312241). RNAscope images were taken using a Zeiss AxioImager Z1 upright microscope with the ZEN software. Immunofluorescence was performed on deparaffinized and rehydrated 7 μm tissue sections. Antigen retrieval was carried out by heating slides in a pressure cooker (121 °C) for 20 min at pH 9.0 (S2367, DAKO). The following primary antibodies were used: chicken anti-eGFP (1:2,000, Abcam ab290), rabbit anti-vimentin (1:500, Abcam ab92547), mouse anti-E-cadherin (1:200, BD Transduction Laboratory 61018). The secondary antibodies used were: anti-chicken/rabbit/mouse Alexa 488/568/647 IgG (1:500, Invitrogen). Images were taken on the Olympus FV3000 inverted confocal microscope.

Generation of mouse cell lines. Embryos were collected at E14.5 and primary dermal fibroblasts were derived from embryonic back skin explants, and primary NPCs were isolated from brain cortices. Primary fibroblasts were immortalized via SV40 large T antigen retroviral infection using standard protocol (pBABE-neo largeTcDNA, Addgene plasmid 1780). SV40-immortalized mouse fibroblasts-SUPERTOPFLASH (STF) were generated with the insertion of 7xTcf-firefly luciferase by retroviral infection using standard protocol (7TFP, Addgene plasmid 24308). For NPC derivation, cortices were first excised from whole brains and mechanically dissociated using a pipette. Cells were cultured as suspension in NPC medium: DMEM/F12 (Gibco 11320) containing 1 × N-2 supplement (ThermoFisher Scientific 17502001), 1 × B-27 supplement (ThermoFisher Scientific 17504001), 2 mM L-glutamine (ThermoFisher Scientific 25030081), 0.1 mM NEAA (Gibco 1140-050), 20 ng ml^{-1} FGF-2 (R&D Systems 233-FB) and 20 ng ml^{-1} EGF (R&D Systems 236-eg). NPCs in suspension were passaged with accutase (Merck Millipore SCR005) every 4–5 days. For adherent cultures, NPCs were plated onto Matrigel-coated (Corning 354231) plates in NPC medium. Adherent mouse NPCs were reprogrammed by transduction of human *OCT4* (also known as *POU5F1*), *SOX2*, *KLF4* and *MYC* (Addgene plasmids 17225, 17226, 17227 and 18119)[37] using standard protocol. After 4 days, transduced cells were reseeded onto irradiated mouse embryonic fibroblasts in mouse iPS cell medium: knockout-DMEM (ThermoFisher Scientific 1029018) supplemented with 10% Knock Out Serum Replacement (ThermoFisher Scientific 10828028), 10% FBS (ThermoFisher Scientific 16000044), 0.1 mM 2-mercaptoethanol (ThermoFisher Scientific 21985023), 2 mM L-glutamine (ThermoFisher Scientific 25030081), 0.2 mM NEAA (ThermoFisher Scientific 1114050) and 1,000 U ml^{-1} mouse LIF (Stem Cell Technologies 78056). iPS cell colonies were picked between days 7 and 15 and maintained in mouse iPS cell medium for expansion on gelatin-coated plates.

Cell treatment with recombinant proteins. For WNT signalling response experiments, immortalized fibroblasts were treated for 24 h in serum-free medium with 25 ng ml^{-1} recombinant WNT3A (R&D Systems 5036-WN), and/or 400 ng ml^{-1} recombinant RSPO1 (4645-RS), RSPO2 (3266-RS), RSPO3 (3500-RS) or RSPO4 (4575-RS) re-suspended in PBS containing 0.1% BSA.

siRNA experiments. siGENOME SMARTpool mouse *Rspo2* (Dharmacon 239405), *Rspo3* (72780), *Znrf3* (407821) or negative control (D-001206-14-05) siRNAs were used to transfect SV40-immortalized mouse fibroblasts. The transfection of 37.5 nM siRNA was performed with Lipofectamine RNAiMAX (Invitrogen 13778-075) or DharmaFECT (Dharmacon T-2001) transfection reagents according to manufacturer protocols.

qPCR experiments. For qPCR experiments, embryonic organs or culture cells were lysed in the QIAGEN RLT buffer and total RNAs were extracted using the QIAGEN RNeasy Mini kit (74106), including the optional DNase RNase-free treatment. cDNAs were obtained using the iScript reverse transcription supermix (Bio-Rad 170-8841). qPCR were performed with primers described in Extended Data Table 2c using the Power SYBR Green Master mix (Applied Biosystems 4367659) on the Applied Biosystems 7900HT Fast Real-Time PCR system. Plotted are data relative to *Actb* and to the control condition. Data are the average of at least three biological triplicates and statistical analyses were done with the PRISM5 software using a one-way ANOVA test with Bonferroni correction for multiple hypothesis testing when more than two groups were compared, or an unpaired *t*-test with Welch's correction when less than three groups were compared.

Xenopus tropicalis experiments. All experiments on *X. tropicalis* were executed in accordance with the guidelines and regulations of Ghent University, faculty of Sciences, Belgium. Approval was obtained by the ethical committee of Ghent University, faculty of Sciences (permit number EC2017-093). No statistical method was used to predetermine sample size. No randomization or blinding was used during the experimental procedures.

***Xenopus tropicalis* whole-mount in situ hybridization.** Probes for *rnf43* and *znrf3* were designed by amplifying the coding sequence by PCR with primers linked to RNA-polymerase sites (Supplementary Table 1). Sense and antisense RNA probes were generated by in vitro transcription with the appropriate RNA polymerase and digoxigenin-rUTP-label. Whole-mount in situ hybridization was carried out as previously described[40]. Imaging was performed with a Leica MZ FLIII stereomicroscope/Leica DC300F camera.

Generation of *X. tropicalis* mosaic mutants by TALEN or CRISPR–Cas9. TALENs were generated using the Golden Gate Cloning protocol as previously described[41] and yields were quantified by Nanodrop (ThermoFischer Scientific). Embryos (two-cell stage) were injected unilaterally with 75 pg rnf43-TALEN-ELD, rnf43-TALEN-KKR, znrf3-TALEN-ELD and znrf3-TALEN-KKD (Extended Data Table 2e). Guide RNA targeting *rspo2* (Extended Data Table 2e) was designed with CRISPRScan (http://www.crisprscan.org/) and generated as previously described[42,43], and yield was quantified by Qubit BR RNA assay (ThermoFischer Scientific). Embryos were injected unilaterally at the two-cell stage with 47 pg *rspo2* gRNA and 900 pg NLS-Cas9-NLS (VIB/UGent Protein Service Facility). Both male and female animals were included in the study once they passed Nieuwkoop stage 59 and were scored as normal, or displaying either amelia (absence of at least one limb) or polymelia (at least one limb showing signs of duplication) by stereomicroscopic examination of limbs. For quantitative analysis of genome editing, nine embryos per injected clutch were pooled and lysed overnight in lysis buffer (50 mM Tris pH 8.8, 1 mM EDTA, 0.5% Tween-20, 200 μg ml^{-1} proteinase K) at 55 °C. Genotyping PCRs were performed with the respective primer pairs shown in Extended Data Table 2f. Targeted deep sequencing of amplicons was performed as previously described and analysed by the BATCH-GE software package[44]. Indel frequency data and sequence variants for all targeted deep sequencing are shown in Supplementary Table 1.

Skeletal staining of *X. tropicalis* tadpoles and froglets. For staining of the skeleton of the mutant animals, premetamorphic tadpoles and postmetamorphic froglets were euthanized using a 0.05% benzocaine solution. Animals were fully eviscerated, skinned and eyes were removed. Whole-mount alcian blue and alizarin red staining was performed as follows: 95% ethanol (4 days, change after 24 h), 100% acetone (48 h), 0.15% alcian blue 8GX (Sigma-Aldrich A3157) in 76% ethanol/20% glacial acetic acid/4% H_2O (24 h), 70% ethanol (24 h), 95% ethanol (12 h), 1% KOH (6 h), 0.05% alizarin red S (Sigma-Aldrich A5533) in 1% KOH (48 h), 1% KOH (48 h). Imaging was performed with a Leica MZ FLIII stereomicroscope/Leica DC300F camera.

Reporting summary. Further information on experimental design is available in the Nature Research Reporting Summary linked to this paper.

Data availability. The data that support the findings of this study are available within the paper or from the corresponding authors upon reasonable request. The whole exome sequencing data for family 1, and the SNP-array data for F3-II:1 shown in Extended Data Fig. 1 have been deposited in the NCBI Gene Expression Omnibus (GEO) database under accession numbers SRP136052 and GSE111781, respectively.

36. Wang, D. et al. Structural basis for R-spondin recognition by LGR4/5/6 receptors. *Genes Dev.* **27**, 1339–1344 (2013).
37. Peng, W. C. et al. Structure of stem cell growth factor R-spondin 1 in complex with the ectodomain of its receptor LGR5. *Cell Reports* **3**, 1885–1892 (2013).
38. Li, S. J. et al. Loss-of-function point mutations and two-furin domain derivatives provide insights about R-spondin2 structure and function. *Cell. Signal.* **21**, 916–925 (2009).

39. Krug, U., Patzschke, R., Zebisch, M., Balbach, J. & Sträter, N. Contribution of the two domains of *E. coli* 5′-nucleotidase to substrate specificity and catalysis. *FEBS Lett.* **587**, 460–466 (2013).
40. Monsoro-Burq, A. H. A rapid protocol for whole-mount in situ hybridization on *Xenopus* embryos. *CSH Protoc.* **2007**, pdb.prot4809 (2007).
41. Van Nieuwenhuysen, T. et al. TALEN-mediated apc mutation in *Xenopus tropicalis* phenocopies familial adenomatous polyposis. *Oncoscience* **2**, 555–566 (2015).
42. Naert, T., Van Nieuwenhuysen, T. & Vleminckx, K. TALENs and CRISPR/Cas9 fuel genetically engineered clinically relevant *Xenopus tropicalis* tumor models. *Genesis* **55**, https://doi.org/10.1002/dvg.23005 (2017).
43. Moreno-Mateos, M. A. et al. CRISPRscan: designing highly efficient sgRNAs for CRISPR-Cas9 targeting in vivo. *Nat. Methods* **12**, 982–988 (2015).
44. Boel, A. et al. BATCH-GE: Batch analysis of Next-Generation Sequencing data for genome editing assessment. *Sci. Rep.* **6**, 30330 (2016).

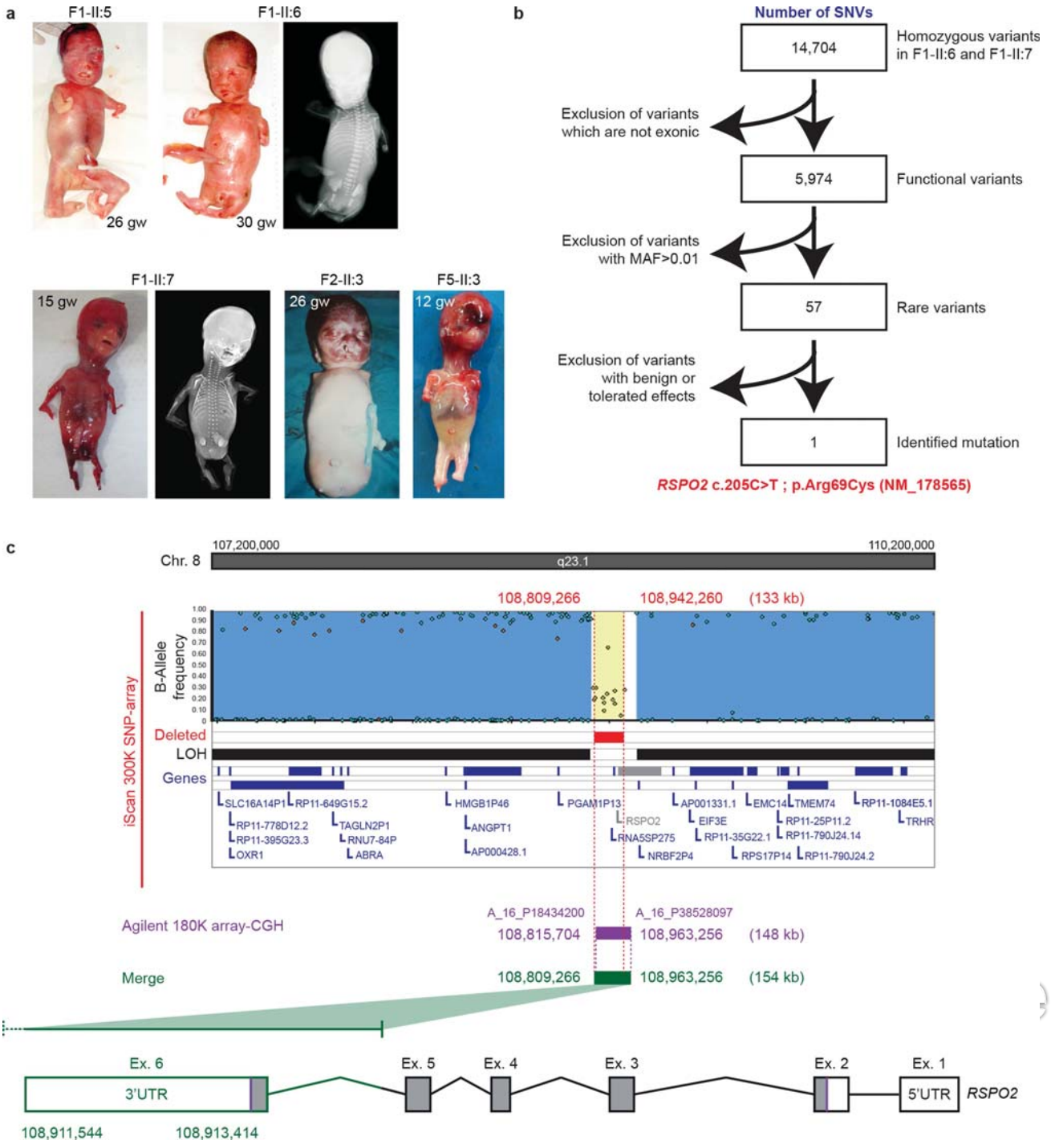

Extended Data Fig. 1 | Pictures of affected fetuses, exome sequencing analysis in family 1 and genotyping analysis in family 3. a, Pictures and radiographs of indicated fetal cases illustrating severe limb defects in fetuses with HFH-RTRD, and the complete absence of limbs in fetuses with TETAMS. **b**, Summary of exome sequencing analysis for family 1, revealing a single biallelic missense mutation in the *RSPO2* gene. **c**, Summary of genotyping in family 3 by SNP-array and array-CGH analysis, revealing a homozygous deletion including exon 6 of *RSPO2*.

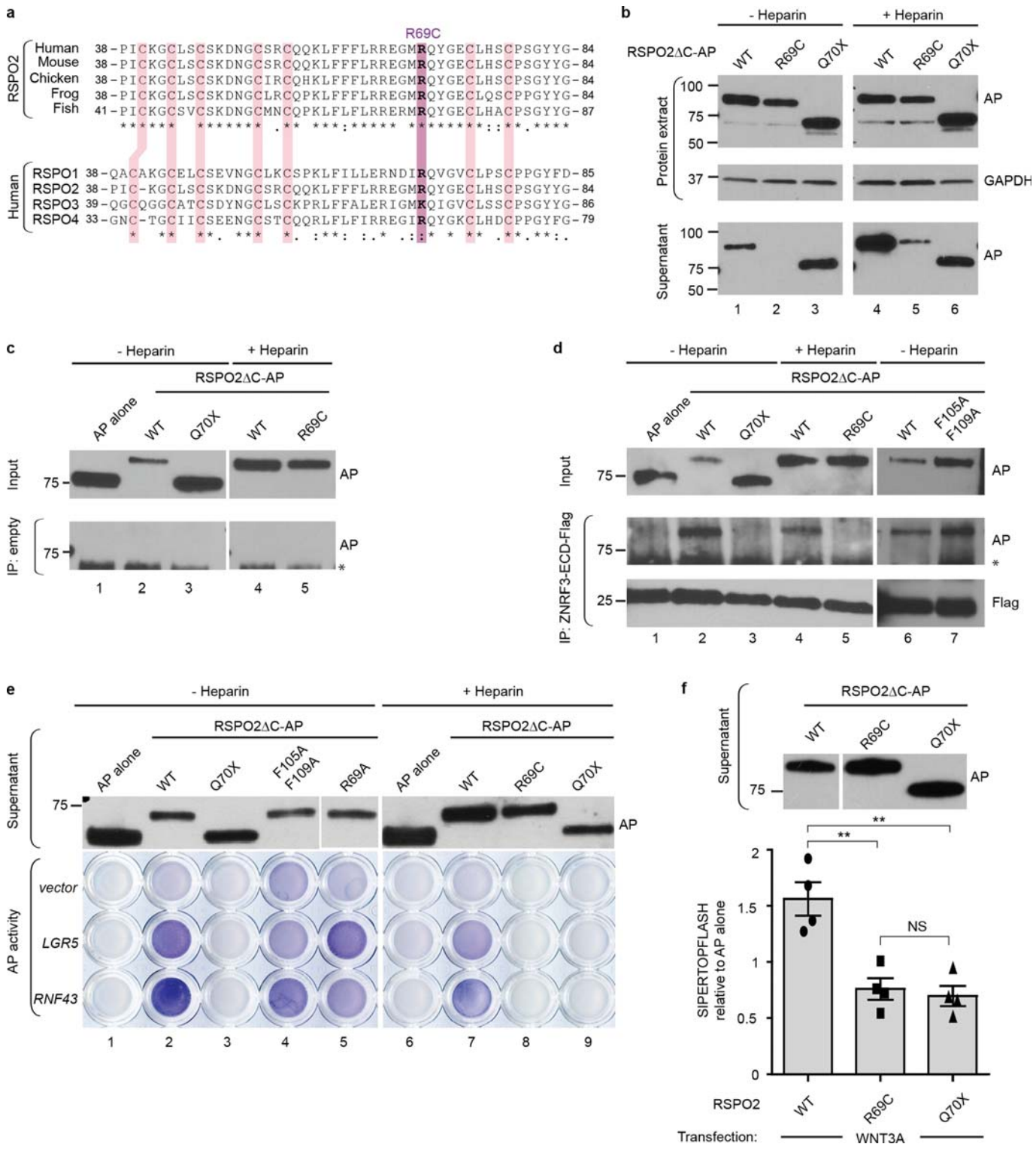

Extended Data Fig. 2 | The RSPO2(R69C) and RSPO2(Q70X) mutants fail to bind ZNRF3. a, The RSPO2 R69 residue (highlighted in purple) is highly conserved in vertebrates and within the human paralogues RSPO1–RSPO4. Conserved cysteine residues of the Furin-like 1 domain are highlighted in pink. Protein alignment performed with ClustalO. **b**, Western blotting of protein extracts and supernatants from HEK293T cells transfected with indicated constructs. Deletion of the RSPO2 C-terminal domain (RSPO2-ΔC) decreases its retention on the cell surface without affecting its receptor binding and WNT enhancement properties[38]. The RSPO2(R69C) mutant was almost undetectable in conditioned media but was greatly increased by the addition of heparin in the medium. **c**, Co-immunoprecipitation of wild-type and mutant forms of RSPO2-ΔC-AP with the ProteinG-Flag beads only. Asterisk indicates an unspecific band. **d**, Co-immunoprecipitation of wild-type and mutant forms of RSPO2-ΔC-AP with the ZNRF3-ECD-Flag E3 ligase. Asterisk indicates an unspecific band. **e**, Cell-surface binding assay of HEK293T cells transfected with empty vector, *LGR5* or *RNF43*, using equivalent amounts of RSPO2-ΔC-AP conditioned media (western blot). Experiments in **b**–**e** were repeated three times. **f**, SUPERTOPFLASH assay in HEK293T-STF cells transfected with WNT3A in the presence of equivalent amounts of RSPO2-ΔC-AP conditioned media (western blot). $n = 4$ biological replicates. Data are mean ± s.e.m. NS, not significant. $^{**}P < 0.01$, one-way ANOVA test with Bonferroni's correction. For gel source data, see Supplementary Fig. 1.

a

Lgr4$^{+/-}$ *Lgr5*$^{+/-}$ *Lgr6*$^{-/-}$ incrosses

Embryos	Expected		Obtained Lgr4		Obtained Lgr5	
n=82	n	%	n	%	n	%
wt	20.5	25	19	23.2	20	24.4
het	41	50	48	58.5	37	45.1
hom	20.5	25	15	18.3	25	30.5

Triple hom	Expected	Obtained
82/16 =	5.125	5

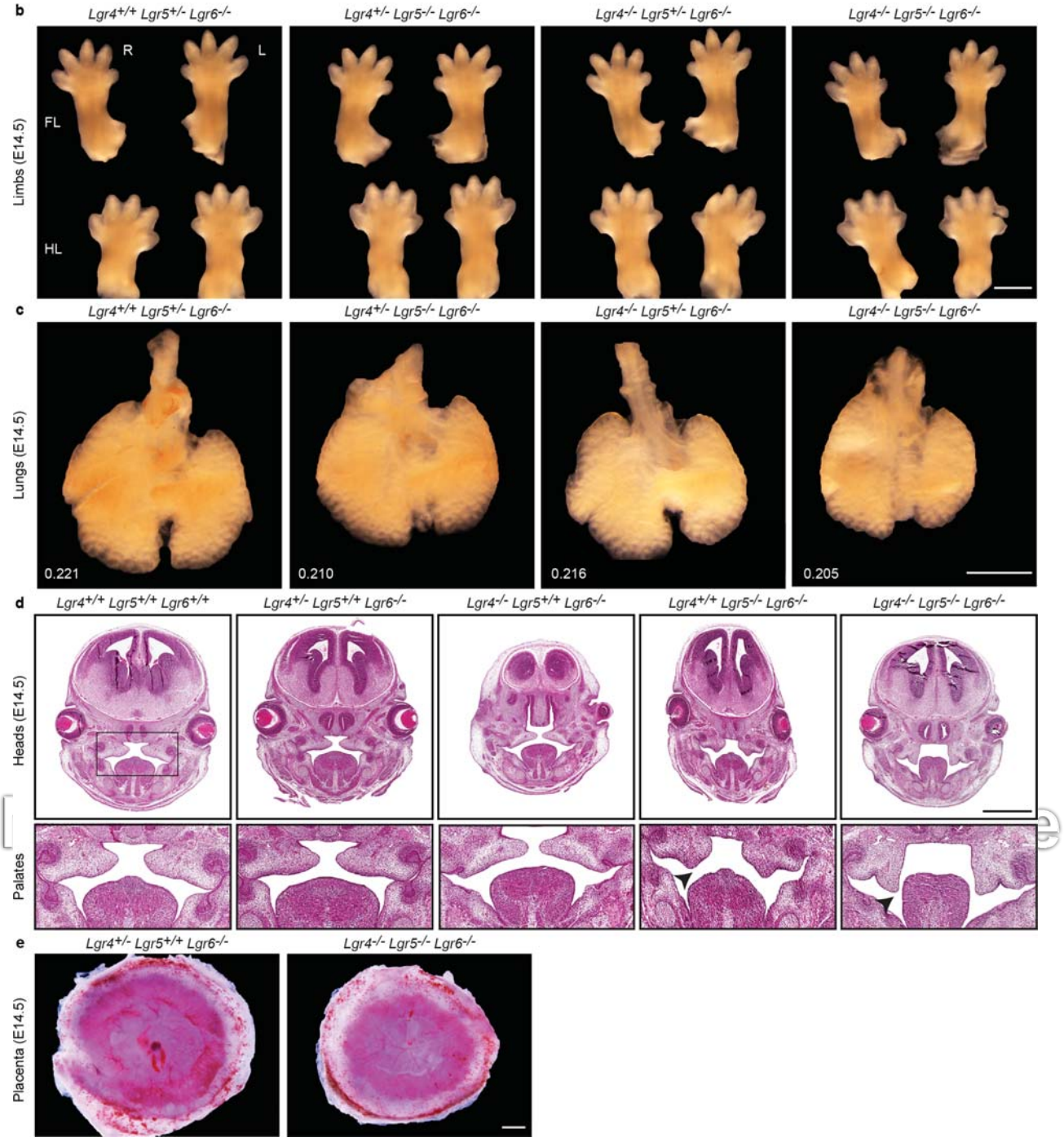

Extended Data Fig. 3 | Mouse *Lgr4/5/6* knock-in embryos do not recapitulate the *Rspo2* and *Rspo3* phenotypes. a, Table indicating the proportion and numbers of analysed embryos. The different genotypes were obtained in Mendelian ratio ($P > 0.05$, χ^2 test). **b**, Normal limbs of embryos with indicated genotypes including a *Lgr4/5/6* triple-knockout embryo. All obtained embryos (see **a**) had a similiar phenotype. FL, forelimbs; HL, hindlimbs; L, left; R, right. Scale bar, 1 mm. **c**, Normal lungs of embryos with indicated genotypes including a *Lgr4/5/6* triple-knockout embryo. Comparable lung length relative to body length is indicated. Scale bar, 1 mm. All obtained embryos (see **a**) had a similiar phenotype. **d**, H&E staining of coronal sections of the heads through the oral cavity. Scale bar, 1 mm. Close-ups of the palatal shelves illustrate the cleft palate present in the *Lgr5/6* double-knockout ($n = 2$) and *Lgr4/5/6* triple-knockout ($n = 2$) embryos (indicated by black arrow heads). **e**, Properly vascularized placenta of a *Lgr4/5/6* triple-knockout embryo compared to a *Lgr6*-knockout embryo. All obtained embryos (see **a**) had a similiar phenotype. Scale bar, 1 mm.

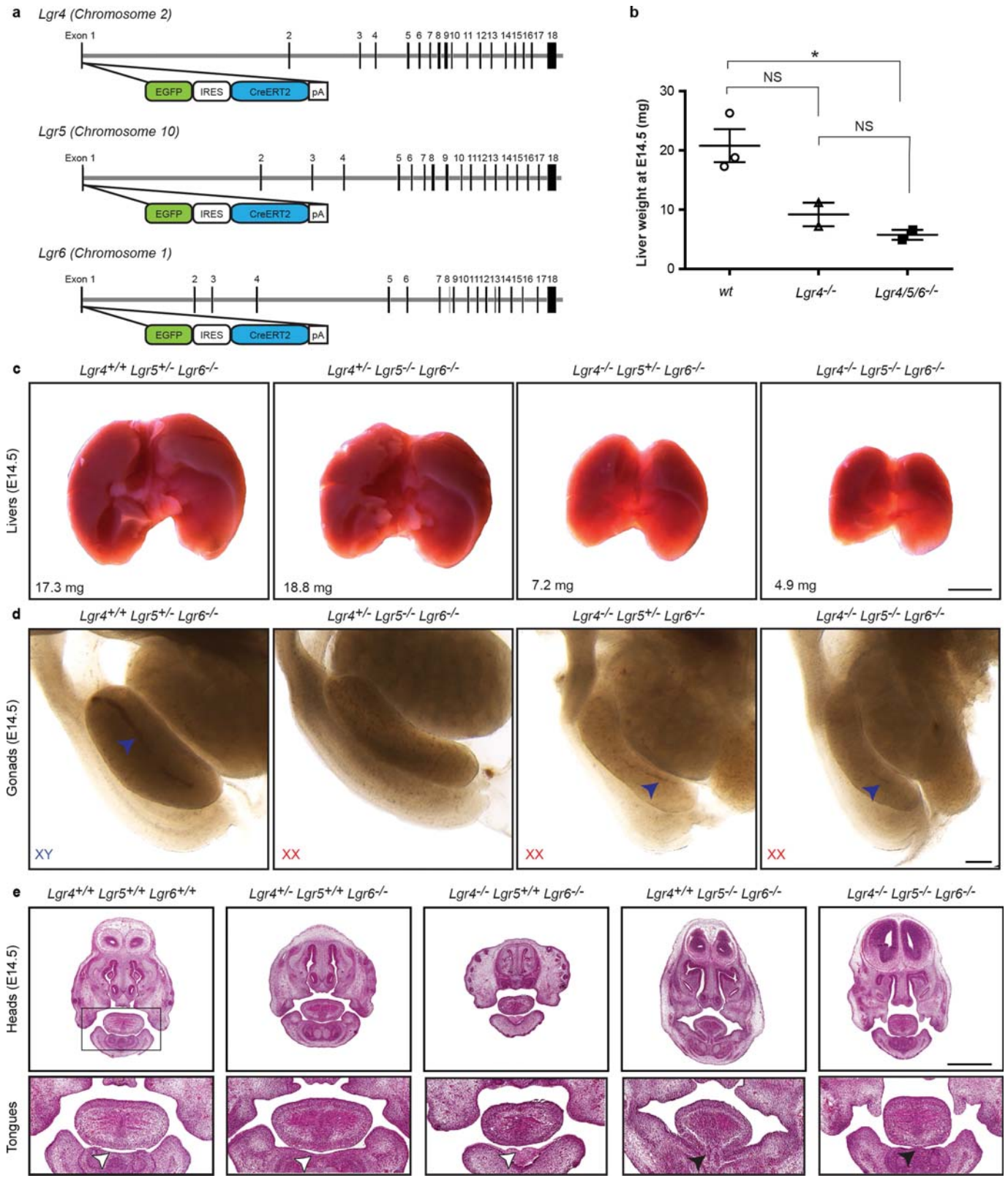

Extended Data Fig. 4 | Mouse *Lgr4*, *Lgr5* and *Lgr6* knock-in embryos recapitulate the knockout phenotypes. a, Illustration of the GFP knock-in in exon 1 of the *Lgr4, Lgr5* and *Lgr6* genes, which cause loss-of-function mutations. **b**, Liver weight in single $Lgr4^{-/-}$ ($n = 2$) and triple $Lgr4/5/6^{-/-}$ ($n = 2$) compared to wild-type ($n = 3$) E14.5 embryos. Data are mean ± s.e.m. NS, not significant. $^*P < 0.05$, one-way ANOVA test with Bonferroni's correction. **c**, $Lgr4^{-/-}$ embryos ($n = 4$) have a smaller liver. Liver weight is indicated. Scale bar, 1 mm. **d**, $Lgr4^{-/-}$ embryos ($n = 2$) show female-to-male sex reversal. Blue arrowheads point to male-specific coelomic vessels. Genetic genders (XY or XX) are indicated. Scale bar, 0.1 mm. **e**, H&E staining of coronal sections of the heads through the oral cavity. Scale bar, 1 mm. Close-ups of the tongue illustrate the ankyloglossia phenotype (tongue attached to the mouth floor, black arrow heads) in $Lgr5^{-/-}$ embryos ($n = 4$), whereas the tongue is detached for other genotypes (white arrowheads).

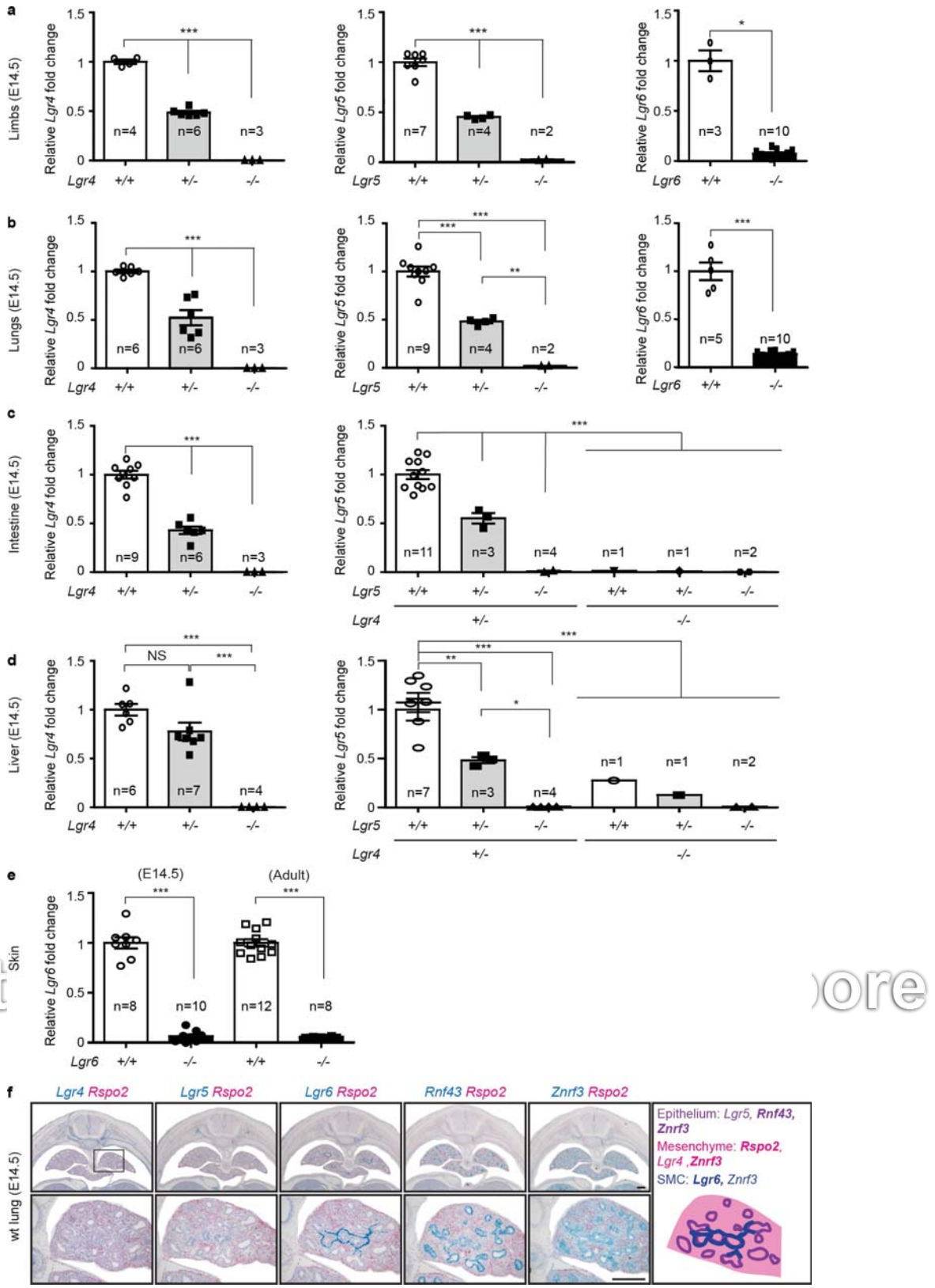

Extended Data Fig. 5 | Mouse *Lgr4*, *Lgr5* and *Lgr6* knock-in cause loss-of-function mutations. a, **b**, qPCR analyses for *Lgr4*, *Lgr5* and *Lgr6* expression in E14.5 limbs (**a**) and lungs (**b**) of wild-type, heterozygous and homozygous mutant embryos for the respective genes. **c**, **d**, qPCR analyses for *Lgr4* and *Lgr5* in embryonic intestine (**c**) and embryonic liver (**d**) of embryos with indicated genotype. **e**, qPCR analyses for *Lgr6* in embryonic and adult skin of wild-type versus homozygous animals. *n* indicates number of embryos. Data are mean ± s.e.m. NS, not significant. $*P < 0.05$, $**P < 0.01$, $***P < 0.001$, one-way ANOVA test with Bonferroni's correction or two-tailed unpaired *t*-test with Welch's correction when less than three groups were compared (for *Lgr6* qPCR analysis). **f**, Duplex RNAscope for the indicated gene (blue) and *Rspo2* (pink) in transverse sections of wild-type E14.5 lungs. Strongly expressed genes are denoted in bold (summary on the right). Scale bars, 0.2 mm. Experiment repeated with three different wild-type embryos.

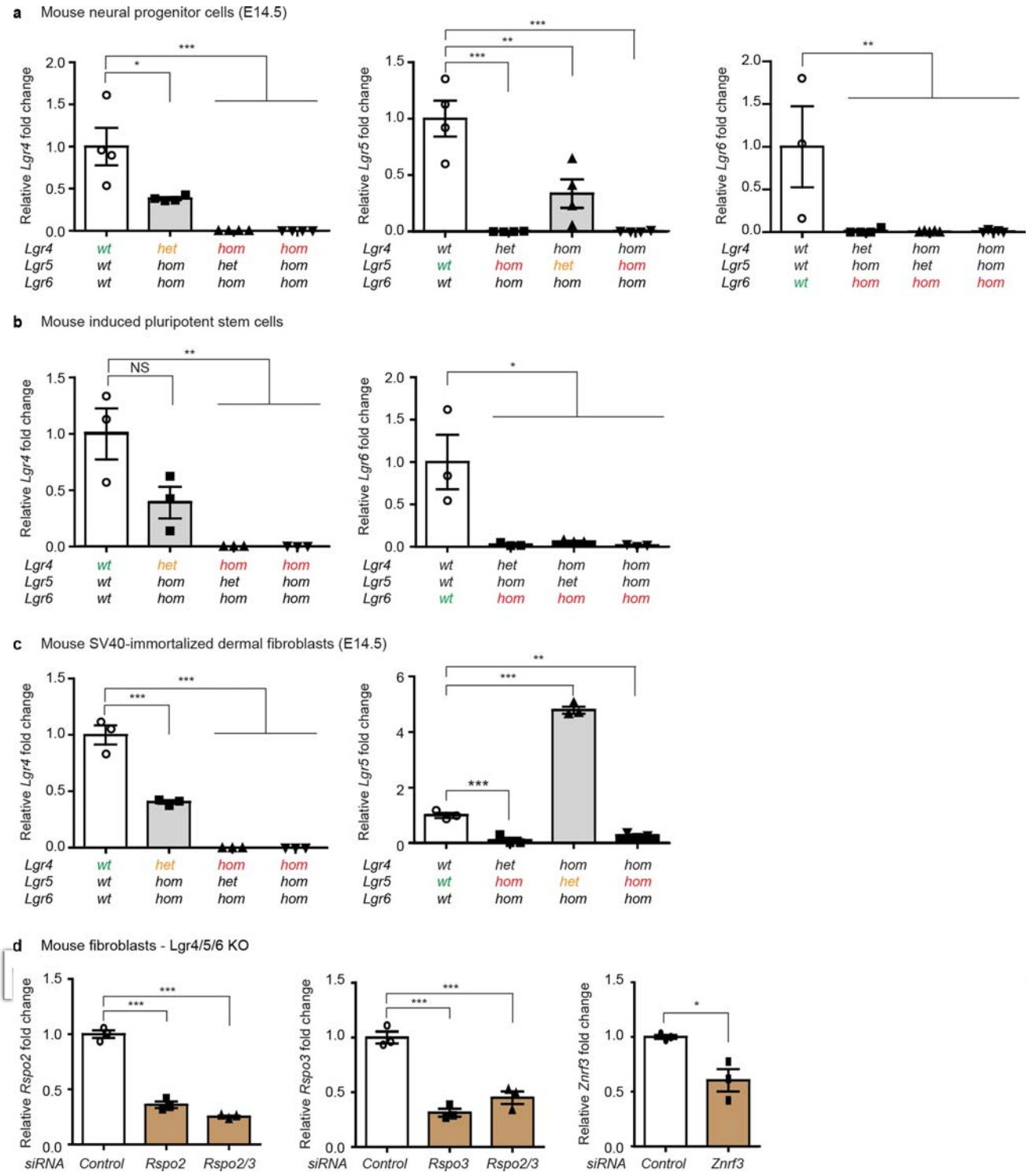

Extended Data Fig. 6 | Expression analyses in cells derived from mutant embryos. a, qPCR analyses for *Lgr4*, *Lgr5* and *Lgr6* in NPCs derived from embryos of indicated genotypes. $n = 4$ biological replicates. **b**, qPCR analyses for *Lgr4* and *Lgr6* in iPS cells derived from NPCs of indicated genotypes. $n = 3$ biological replicates. **c**, qPCR analyses for *Lgr4* and *Lgr5* in SV40-immortalized dermal fibroblasts derived from embryos of indicated genotypes. $n = 3$ biological replicates. **d**, qPCR analyses for *Rspo2*, *Rspo3* and *Znrf3* in *Lgr4/5/6* triple-knockout SV40-immortalized fibroblasts, transfected with indicated siRNAs. $n = 3$ biological replicates. Data are mean ± s.e.m. NS, not significant. $^{*}P < 0.05$, $^{**}P < 0.01$, $^{***}P < 0.001$, one-way ANOVA test with Bonferroni's correction.

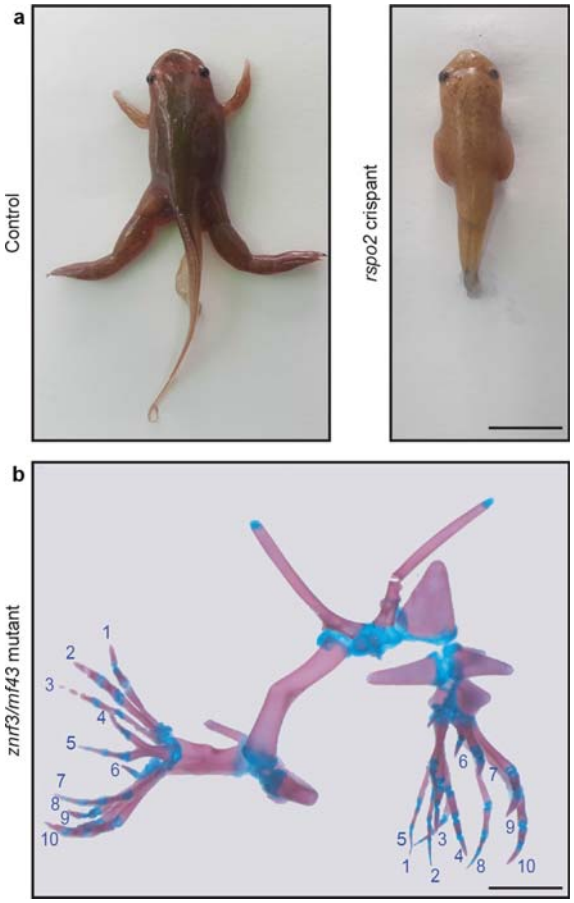

Extended Data Fig. 7 | Extreme phenotypes of *Xenopus tropicalis* mutant tadpoles. a, Control and *rspo2* CRISPR–Cas9-injected tadpole showing a complete tetra-amelia phenotype probably due to incomplete cleavage at the time of injection and leakage of the CRISPR–Cas9 between the two blastomeres ($n = 3$ froglets). Scale bar, 1 cm. **b**, Alizarin red and alcian blue staining of a double-mutant *rnf43/znrf3* TALEN-injected tadpole showing complete mirror-image diplopodia of both hindlimbs with 10 digits each ($n = 4$ froglets). Scale bar, 0.2 cm.

Extended Data Table 1 | Clinical characteristics of affected individuals with biallelic *RSPO2* mutations

	Humero-Femoral Hypoplasia with Radio-Tibial Ray Deficiency				Tetra-amelia syndrome						
	Family 1				Family 2		Family 3	Family 4	Family 5		
	II-3	II-5	II-6	II-7	II-2	II-3	II-1	II-1	II-1	II-2	II-3
Gender	male fetus	female fetus	female fetus	male fetus	male	male fetus	female fetus	female fetus	male fetus	n/a	Female fetus
Termination of pregnancy	30th gw	26th gw	30th gw	15th gw	n/a	26th gw	22nd gw	20th gw	20th gw	13th gw	12th gw
Year of birth	2001	2009	2011	2012	1989	1991	2006	2013	2015	2016	2017
Age at death	n/a	n/a	n/a	n/a	stillbirth	n/a	n/a	n/a	n/a	n/a	n/a
Origin	Turkey				Turkey		Portugal	France		India	
Consanguinity	yes				yes		Not reported	yes		yes	
Case report	This paper				Basaran *et al.*, 1994		Sousa *et al.*, 2008	This paper		This paper	
***RSPO2* cDNA (NM_178565)**	c.205C>T				c.208C>T		154 kb deletion chr8:108,809,266-108,963,256	c.409G>T		c.123delG	
RSPO2 protein (NP_848660)	p.Arg69Cys				p.Gln70*		n/a	p.Glu137*		p.Gly42Valfs*49	
Zygosity	parents are heterozygous	homozygous	homozygous		parents are heterozygous		homozygous	homozygous	homozygous	parents are heterozygous	homozygous
Symmetry of the limb phenotype	+	-	+	-	+	+	+	+	+	+	-
Upper limbs	Short and underdeveloped	Hypoplastic upper limb girdles. Flexion contractures of the elbow joints with pterygia. Short arms with a single tubular bone, ending with a single finger-like appendage with a well-formed nail structure.	Bilateral severely hypoplastic upper extremities with one, markedly thin tubular bone, with bilateral aplasia of thumbs and two finger-like appendages.	Hypoplastic shoulders. On the right: bowed and short humerus, single tubular bone on the forearm, thumb aplasia, ending with two finger like appendages. On the left: short arm with a single tubular bone, ending with a single finger like appendage.	Amelia	Complete absence	Complete absence	Complete absence	Complete absence	Rudimentary appendages	Complete absence of left upper limb, hypoplastic right arm with absence of forearm and hand.
Lower limbs	Short and underdeveloped	Flexion contractures of the elbow joints with pterygia. Mesomelic shortness of the legs with tibial hemimelia. Bilateral clubfeet, bilateral absence of halluces with three toes on the right foot (digit I and digit II missing).	Severely hypoplastic lower limbs with single, markedly thin tubular bone. Two toes on the feet bilaterally.	Hypoplastic pelvis, severely hypoplastic lower limbs with a single tubular bone, three toes on the left and two toes on the right, pes equinovarus.	Amelia	Rudimentary milimetric buds	Complete absence	Rudimentary appendages	Rudimentary appendages	Both femur seen, absence of lower extermities below the knees.	Absence of lower extrimities below the knee.
Others	n/a	Hypoplastic scapulae, a rudimentary triangular bone on the left, diaghragmatic hernia on antenatal ultrasound at the 27th week.	Severely hypoplastic pelvis structure. Prominent glabella, mild retrognathia.	n/a	Cleft lip-palate, no autopsy.	Bilateral cleft lip-palate, bilateral lung agenesis, bilateral palpebral fusion, micrognathia, unfused maxillary processes, severe mandibular hypoplasia, absence of nipples, small penis, absence of scrotum (testes intra-abdominal), heart defects.	Bilateral cleft lip-palate, bilateral lung agenesis, hyperecogenic focus at the right ventricle.	Bilateral cleft lip-palate, microretrognatism. Short frenulum with the tongue tethered to the floor of the mouth (ankyloglossia). Bilateral lung agenesis	Dysmorphic right ear, hypertelorism, bilateral cleft lip, complete cleft palate and severe micrognathia. Short frenulum with the tongue tethered to the floor of the mouth (ankyloglossia). Complete agenesis of both lungs and blind ending main bronchi. Agenesis of branches of pulmonary atery. Hypoplastic pulmonary veins.	Ultrasound examination: Severe micrognathia. Heart fills up most of the chest. Stomach bubble seen.	Severe mirco-retrognathia, unilateral cleft lip (left), posterior cleft palate, glossoptosis. Complete agenesis of both lungs and blind ending main bronchi. Agenesis of branches of pulmonary atery. Hypoplastic pulmonary veins.

n/a, not applicable.

Extended Data Table 2 | List of primers

a Human genotyping primers	
RSPO2-exon2-F	5'-CGGCTCGTGCTAGGCAGT-3'
RSPO2-exon2-R	5'-CAGGGTCCTAAAGGTGGGGA-3'
RSPO2-exon3-F	5'-GACATCCCCATGAGCCA-3'
RSPO2-exon3-R	5'-CACCCAGCAAGCTTAAACT-3'
RSPO2-exon4-F	5'-GTTGAAAGAGACAGGGATGACT-3'
RSPO2-exon4-R	5'-CAGTTCTACTGAACAAGAGAACCA-3'
RSPO2-exon5-F	5'-GGTCTTCAAGGCTGTACCACT-3'
RSPO2-exon5-R	5'-GAAGCACACAGCACACAGT-3'
RSPO2-exon6-F	5'-GGTGATGTTTTCCAGATGGGCT-3'
RSPO2-exon6-R	5'-CTGGGAACAGATACTGGGCA-3'

b Mouse genotyping primers	
Lgr4-WT-F	5'-TGCAACCCTAGAAGGGAAAA-3'
Lgr4-WT-R	5'-CTCACAGTGCTTGGGTGAAG-3'
Lgr4-null-F	5'-GCCTGCATTACCGGTCGATGCAACGA-3'
Lgr4-null-R	5'-CTCACAGTGCTTGGGTGAAG-3'
Lgr5-WT-F	5'-ACATGCTCCTGTCCTTGCT-3'
Lgr5-WT-R	5'-GTAGGAGGTGAAGACGCTGA-3'
Lgr5-null-F	5'-CACTGCATTCTAGTTGTGG-3'
Lgr5-null-R	5'-CGGTGCCCGCAGCGAG-3'
Lgr6-WT-F	5'-CGCTCGCCCGTCTGAGC-3'
Lgr6-WT-R	5'-GCGTCCAGGTCCGCAGG-3'
Lgr6-null-F	5'-CGCTCGCCCGTCTGAGC-3'
Lgr6-null-R	5'-CCTGGACGTAGCCTTCGGGC-3'

c Mouse qPCR primers	
Lgr4-qPCR-F	5'-GCCTTCACCCAAGCACTG-3'
Lgr4-qPCR-R	5'-CAGCCAGTTGTAGCTCCTCT-3'
Lgr5-qPCR-F	5'-ACAACCCCATCCAATTTGTTG-3'
Lgr5-qPCR-R	5'-CGAGGCACCATTCAAAGTCA -3'
Lgr6-qPCR-F	5'-CCCTGACTATGCCTTCCAGA-3'
Lgr6-qPCR-R	5'-ATGCTGGATGCGGTTGTTAT-3'
Rnf43-qPCR-F	5'-GGCCTATGTGTGGATTGAGC-3'
Rnf43-qPCR-R	5'-TGAGGCCAGGATGATCACAA-3'
Znrf3-qPCR-F	5'-CATCCGACTGTGCCATCTGT-3'
Znrf3-qPCR-R	5'-GCCATGGATCCACACACTTC-3'
Axin2-qPCR-F	5'-GAGTGGACTTGTGCCGACTTCA-3'
Axin2-qPCR-R	5'-GGTGGCTGGTGCAAAGACATAG-3'
Rspo1-qPCR-F	5'-ATACTTTGATGCCCGCAACC-3'
Rspo1-qPCR-R	5'-CTCACAGTGCTCGATCTTGC-3'
Rspo2-qPCR-F	5'-CGAGCCCCAGATATGAACAG-3'
Rspo2-qPCR-R	5'-AAAAGCCTACTTTGCACTTCG-3'
Rspo3-qPCR-F	5'-TGTGTCTCTCTTCGTGTCCA-3'
Rspo3-qPCR-R	5'-AGGTATCACAGTCAACTTTGCA-3'
Rspo4-qPCR-F	5'-GGACATGCTCGCCCTGTA-3'
Rspo4-qPCR-R	5'-GAACAGCCATTCTCCTCCGA-3'
Actin-qPCR-F	5'-AAGGCCAACCGTGAAAAGAT-3'
Actin-qPCR-R	5'-GTGGTACGACCAGAGGCATAC-3'

d Target sequences for *Xenopus tropicalis* rnf43 and znrf3 TALENs, and rspo2 gRNA	
Xt_rnf43-TALEN-ELD	5'-TGCTCACGGTGACTCTC-3'
Xt_rnf43-TALEN-KKR	5'-CCATGGGCACCACGGAA-3'
Xt_znrf3-TALEN-ELD	5'-TTTTTCGTGGTGGTGTC-3'
Xt_znrf3-TALEN-KKR	5'-CTCCTTATCAAGATCAA-3'
Xt_rspo2-gRNA	5'-TGACTCCATAGTATCCAGGAGGG-3'

e PCR primers for *Xenopus tropicalis in situ* probes	
Xt_znrf3-insitu-F	5'-AATTAACCCTCACTAAAGGG**GCTGTGATATTTGATGTGTCTG-3'**
Xt_znrf3-insitu-R	5'-TAATACGACTCACTATAGGG**ACTTCCACCAACCTCCTG-3'**
Xt_rnf43-insitu-F	5'-AATTAACCCTCACTAAAGGG**GGCTTCATTTCCATTGTCAAACTG-3'**
Xt_rnf43-insitu-R	5'-TAATACGACTCACTATAGGG**TCCTGCCCATCTGTGAACTC-3'**

f *Xenopus tropicalis* genotyping primers	
Xt_rnf43-F	5'-CCACACCCCAACAAAATCA-3'
Xt_rnf43-R	5'-CCACACCCCAACAAAATCA-3'
Xt_znrf3-F	5'-ACAGCATGCCTTCCCTACAC-3'
Xt_znrf3-R	5'-GTAGGTTGCTGCCAAATCTCAC-3'
Xt_rspo2-F	5'-GTCGTGTTGAAATGGTGCGG-3'
Xt_rspo2-R	5'-GTTCCTTGACAAGTATCCAAGCTG-3'

a, Genotyping primers for human *RSPO2*. **b**, Genotyping primers for mouse *Lgr4, Lgr5* and *Lgr6* wild-type and knock-in alleles. **c**, Mouse qPCR primers used in this study. **d**, Target sequences for *X. tropicalis rnf43* and *znrf3* TALENs, and *rspo2* gRNA. **e**, PCR primers for *X. tropicalis* in situ probes via cloning-free methodology. **f**, Genotyping primers for *X. tropicalis rnf43* and *znrf3* TALENs, and *rspo2* CRISPR–Cas9 target sites.

nature research

Corresponding author(s): Bruno REVERSADE

Life Sciences Reporting Summary

Nature Research wishes to improve the reproducibility of the work that we publish. This form is intended for publication with all accepted life science papers and provides structure for consistency and transparency in reporting. Every life science submission will use this form; some list items might not apply to an individual manuscript, but all fields must be completed for clarity.

For further information on the points included in this form, see Reporting Life Sciences Research. For further information on Nature Research policies, including our data availability policy, see Authors & Referees and the Editorial Policy Checklist.

Please do not complete any field with "not applicable" or n/a. Refer to the help text for what text to use if an item is not relevant to your study.
For final submission: please carefully check your responses for accuracy; you will not be able to make changes later.

Experimental design

1. Sample size

Describe how sample size was determined.

No statistical method was used to predetermine sample size.

Human: we obtained 5 families with 4 different mutations in RSPO2 with similar phenotypes.

Mouse: For the PORCN inhibition treatment, we obtained a total of 46 embryos, all showing limb and lung defects. For the Lgr mutants, we aimed at analysing at least n=3 triple Lgr4/5/6 KO embryos and managed to obtain n=5.

Xenopus: more than 20 froglets were obtained for each type of mutant (Rspo2 or Znrf3/Rnf43), all showing similar phenotypes.

2. Data exclusions

Describe any data exclusions.

No data was excluded.

3. Replication

Describe the measures taken to verify the reproducibility of the experimental findings.

All experiments were performed with at least three biological triplicates. All attempts at replication were successful.

4. Randomization

Describe how samples/organisms/participants were allocated into experimental groups.

Samples were allocated into experimental groups according to their genotype.

5. Blinding

Describe whether the investigators were blinded to group allocation during data collection and/or analysis.

The investigators were not blinded to group allocation during data analysis. Samples or animals were grouped by their genotype / treatment.

Note: all in vivo studies must report how sample size was determined and whether blinding and randomization were used.

6. Statistical parameters

For all figures and tables that use statistical methods, confirm that the following items are present in relevant figure legends (or in the Methods section if additional space is needed).

n/a	Confirmed
☐	☒ The exact sample size (*n*) for each experimental group/condition, given as a discrete number and unit of measurement (animals, litters, cultures, etc.)
☐	☒ A description of how samples were collected, noting whether measurements were taken from distinct samples or whether the same sample was measured repeatedly
☐	☒ A statement indicating how many times each experiment was replicated
☐	☒ The statistical test(s) used and whether they are one- or two-sided *Only common tests should be described solely by name; describe more complex techniques in the Methods section.*
☐	☒ A description of any assumptions or corrections, such as an adjustment for multiple comparisons
☐	☒ Test values indicating whether an effect is present *Provide confidence intervals or give results of significance tests (e.g. P values) as exact values whenever appropriate and with effect sizes noted.*
☐	☒ A clear description of statistics including central tendency (e.g. median, mean) and variation (e.g. standard deviation, interquartile range)
☐	☒ Clearly defined error bars in all relevant figure captions (with explicit mention of central tendency and variation)

See the web collection on statistics for biologists for further resources and guidance.

Software

Policy information about availability of computer code

7. Software

Describe the software used to analyze the data in this study.

Burrows-Wheeler Aligner (BWA package version 0.6.2) was used to map the whole-exome data to the human genome (hg19). Further alignment manipulations were performed by Samtools (version 0.1.18). Base quality (Phred scale) scores were recalibrated using GATK's covariance recalibration for each sample (Oxford Gene Technology), and variant calling was performed using ANNOVAR tool. All the alterations were browsed on OGT NGS (Oxford Gene Technologies' Next Generation Sequencing) and IGV (Integrated Genomic Viewer) browsers.

Mutations in Xenopus were analysed by targeted deep sequencing with the BATCH-GE software package.

GraphPad Prism was used to statistically analyze the data.

For manuscripts utilizing custom algorithms or software that are central to the paper but not yet described in the published literature, software must be made available to editors and reviewers upon request. We strongly encourage code deposition in a community repository (e.g. GitHub). *Nature Methods* guidance for providing algorithms and software for publication provides further information on this topic.

Materials and reagents

Policy information about availability of materials

8. Materials availability

Indicate whether there are restrictions on availability of unique materials or if these materials are only available for distribution by a third party.

All materials used in this study are available for distribution upon request.

9. Antibodies

Describe the antibodies used and how they were validated for use in the system under study (i.e. assay and species).

Antibodies used for Western Blotting:
*anti-Alkaline Phosphatase (AP), GenHunter #Q310 (used for Western blot analysis of AP-tagged proteins from cell extracts and culture media, tested by the manufacturer on 293T overexpressing AP itself or AP fusion proteins)
*anti-FLAG M2, Cell Signaling #14793S (commonly used for Western blot analysis of FLAG-tagged proteins, tested by the manufacturer on 293T cells transfected or not with FLAG-tagged proteins)
*anti-GAPDH, SantaCruz #47724 (commonly used for Western blot analysis of GAPDH expression in human samples, tested by the manufacturer in U-87 MG and SK-BR-3 whole cell lysates, cited more than 500 times)

Antibody used for immunoprecipitation:
*anti-FLAG M2, Sigma #F3165 (commonly used to immunoprecipitate FLAG-tagged proteins, cited more than 1000 times)

10. Eukaryotic cell lines

a. State the source of each eukaryotic cell line used.
HEK293T and HEK293T-STF cells are from ATCC.

b. Describe the method of cell line authentication used.
The cell lines were not authenticated.

c. Report whether the cell lines were tested for mycoplasma contamination.
All cell lines were tested negative for mycoplasma contamination.

d. If any of the cell lines used are listed in the database of commonly misidentified cell lines maintained by ICLAC, provide a scientific rationale for their use.
No commonly misidentified cell lines were used.

Animals and human research participants

Policy information about studies involving animals; when reporting animal research, follow the ARRIVE guidelines

11. Description of research animals

Provide all relevant details on animals and/or animal-derived materials used in the study.
C57 BL/6 mouse embryos were analysed at E14.5 and E18.5.
Xenopus tropicalis froglets were analysed at stages 50 to 66.

Policy information about studies involving human research participants

12. Description of human research participants

Describe the covariate-relevant population characteristics of the human research participants.
This study involves the participation of families with male and female foetuses presenting with limb defects.